Models of sapwood area vertical distribution in lodgepole pine and western hemlock in western Canada.

Keywords

Sapwood area, tree crown and stem, pipe model theory, *Pinus contorta, Tsuga heterophylla*.

Abstract
Mixed-effects models described sapwood area distribution along stems of 60 lodgepole pine and 124 western hemlock trees. The Gallant-Fuller segmented polynomial model (GF) for stem taper equations comprising three joined polynomial segments, and a functional components model (FC) derived from pipe model theory containing three additive components were compared. A fixed effects model was constructed and then random tree effects were added. Random effect variability was highest at the tree base for both models and species. Random variation was regressed against tree-level measurements to identify additional fixed effect crown or height variables. All models fit well, but root mean square error (RMSE) was lower for pine than hemlock, and lower for the FC than GF final fixed effect model. Sapwood area conformed to pipe model theory assuming variable stem permeability that was associated with tree crown and total height. Pine validation data from four Alberta and two British Columbia sites showed the FC model underpredicted (9%) and the GF model overpredicted (7%) sapwood area mainly in the lower stem. Reasonable predictions of sapwood area could be derived from ground-based or remote sensing methods allowing classification of sites, trees, and logs based on this wood quality characteristic.

Introduction

Sapwood tissue conducts water and nutrients from the roots to the foliage, and provides storage for both water and metabolites. It is distinguished from heartwood by higher moisture content, lower chemical extractive content, and a cell microstructure that favors the flow of liquid water. The boundary between sapwood and heartwood gradually advances into the sapwood with time, but the process by which sapwood is transformed into heartwood is not well understood (Bamber and Fukazawa 1985). The transformation involves the death of ray parenchyma cells, possibly caused by a rapid increase in the content of toxic extractives (Taylor et al. 2002; Bergström 2003).

The differing characteristics of sapwood and heartwood affect the processing and value of forest products (Panshin and de Zeeuw 1970, p. 474, 478). Moisture content must be taken into account in drying schedules for solid wood to avoid warping. Solid wood products consisting entirely of sapwood or heartwood are more homogeneous than products that include both types of wood. The superior hydraulic conductivity of sapwood allows better uptake of liquid-borne wood treatments. On the other hand, the lower chemical extractive content of sapwood makes it less resistant to decay organisms, resulting in reduced durability of wood products (Taylor et al. 2002). In pulping, the higher extractive content of heartwood can necessitate additional treatment to achieve desired whiteness. In some species, color differences between heartwood and sapwood lead to differentiation of wood products based on appearance.

In accordance with pipe model theory (Shinozaki et al. 1964), the amount and distribution of sapwood in tree stems is closely related to the amount and distribution of foliage in the crown (Waring et al. 1982). The relationship between sapwood cross-sectional area and foliage mass is sufficiently strong such that it is widely used to predict foliage mass from sapwood cross-sectional area (e.g., Gilmore et al. 1996). Sapwood cross-sectional area at the base of the live crown is used in these relationships, because sapwood area continues to increase below the crown (Waring et al. 1982; Dean and Long 1986). The increase in sapwood area with distance below the crown is coincident with a decrease in longitudinal permeability, combining to result in nearly constant hydraulic conductance along the stem (Booker and Kininmonth 1978; Shelburne and Hedden 1996).

The general pattern of the distribution of sapwood area along the tree stem is an increase from the apex of the tree downward (Long et al. 1981; Mörling and Valinger 1999; DeBell and Lachenbruch 2009). In the uppermost part of the tree stem, the xylem is entirely sapwood; heartwood typically begins to appear well above the base of the live crown. Sapwood area increases rapidly near the stem base, and is larger at wide tree spacings, presumably because these trees have larger crowns (Mörling and Valinger 1999; DeBell and Lachenbruch 2009). Correspondingly, sapwood area at breast height increases with tree diameter, age and radial growth rate (Sellin 1994). Knowledge of sapwood distribution in stems is valuable not only for understanding tree physiological processes, but also for optimal use of sapwood and heartwood in forest products. Optimization along the entire forest product value chain from forest to market is possible for sapwood or heartwood inventories. An attempt to estimate heartwood percentage in *Pinus sylvestris* stems from site,

stand, and tree variables available in forest inventory was unsuccessful (Björklund 1999), possibly because the crown variables were limited to crown length, or the model form was unsuitable.

The extensive evidence for the pipe model theory implies that tree hydraulic function could provide a sound basis for models of sapwood area distribution along the stem. Dean and Long (1986) explained most of the variation in *Pinus contorta* sapwood area using leaf area and distance from the crown midpoint as independent variables. A functional approach may not be necessary to model sapwood area relations. Maguire and Batista (1996) successfully described stem sapwood area using models originally developed for stem taper. Their sapwood area models require dbh, total height and height to crown base. In a related approach, Ojansuu and Maltamo (1995) estimated sapwood area as the difference between simultaneous stem and heartwood taper models.

The overall aim of this study was to develop models using variables obtainable from remote sensing, such as tree height and crown dimensions, to describe the longitudinal sapwood distribution in lodgepole pine [*Pinus contorta* (Doug. Ex. Loud.)] and western hemlock [*Tsuga heterophylla* (Raf.) Sarg.]. These two species are abundant in western Canada and have contrasting ecological requirements (Farrar 1995). Specific objectives were (i) to assess whether functional models have greater descriptive ability than purely empirical models, and (ii) to assess the predictability of models by applying models to a separate region.

Materials and Methods

Data for model development

Data from sample trees represented a wide range of tree (Table 1) and plot (Table 2) characteristics. Sapwood area and tree attributes were obtained from data previously collected by the British Columbia Ministry of Forests, Lands and Natural Resource Operations (BCMFLNR) (Fig. 1). Lodgepole pine trees [*Pinus contorta* (Doug. Ex. Loud.)] were selected from two geographic locations near Kamloops BC (KM 50.44N, 120.55W) and another two locations near Quesnel BC (QS 53.00N, 121.99W). Western hemlock trees [*Tsuga heterophylla* (Raf.) Sarg.] were also selected in BC locations near Adams Lake (AD, 50.40N, 126.20W), Cowichan Lake (CW, 48.78N, 124.13W), Port McNeill (PN, 50.57N, 127.17W), Mission (MI, 49.20N, 122.30W), Port Renfrew (PR, 48.59N, 124.29W), and at the Malcolm Knapp Research Forest maintained by the University of British Columbia (UB, 49.28N, 122.57W). These species are referred to as pine and hemlock hereafter. Trees encompassed a range of diameters and crown classes in each stand (i.e., dominant, codominant, intermediate and overtopped). Open grown trees from the same stand were included to expand the range of crown conditions. Trees were restricted to those free of defects or damage from pests, diseases or abiotic causes and disks to 0.3 m and above. Further description is found in Mansfield et al. (2007) and Nemec et al. (2012).

Prior to felling, a fixed-area plot including about 30 neighbors was established around each sample tree to describe the neighborhood. The crown projection area was mapped by measuring the radial distance from the tree stem to the perimeter of the crown at several

points around the tree. Cross-sectional disks were cut at heights of 0.3 m, 0.7 m, 1.3 m, and at six-to-ten additional locations equally spaced between 1.3 m and the tree top. The transition between heartwood and sapwood was visually determined based on wood color differences (Panshin and de Zeeuw 1970) and measured on two radii per disk. Color difference is distinct in pine, and though less so in hemlock, was still estimable after wetting the surface with water and observing the difference in adhesion of a water soluble pencil across the sapwood to heartwood boundary. Radius positions were determined by measuring the outside bark diameter and subtracting the average bark thickness from half of this diameter, and then marking this length on the disk. The sapwood area is the difference between the inside bark area and heartwood area, with areas determined from the corresponding radius and the formula for the area of a circle.

Pine validation data sets

Validation data were obtained from four sites in Alberta [MacKay (MK, 53.55N, 115.53W, 862m), McCardell (MC, 53.2N, 115.18W, 1408m), Teepee Pole Flat (TF, 51.9N, 115.18W,1472m), and Teepee Pole North (TN, 53.87N, 115.17W, 1409m)] and two sites in BC [Parsons (PS, 51N, 116.7W, 1152m) and Cranbrook (CB, 49.4N, 115.6W, 1339m)] (Fig. 1). The Alberta sites are long-term pine juvenile thinning trials with various initial basal areas ranging from 2 to 26 m^2/ha, and up to 41 m^2/ha in the unthinned control plots, all established between 42 and 55 years before measurement. The BC sites are long-term commercial thinning trials, with basal area ranging from 11 to 21 m^2/ha in thinned plots and up to 46 m^2/ha in control plots at establishment 16 years before measurement.

For all sites, stem diameter at breast height (1.3 m) and tree height was measured for every tree. Live crown height was measured from the ground level to the base of the continuous live crown defined by a whorl with more than two branches with green leaves. Crown radius was the distance from the center of the tree bole to the edge of the crown margins (drip zone) averaged over four cardinal directions. Stem disks were cut at 30 cm (stump height), 130 cm (breast height), at 1/3 and 2/3 of the distance between breast height and the merchantable top of 7.5 cm diameter, at the internode below the lowest live branch, at the base of the live crown, at the most vigorous part of the live crown, and at the merchantable top. Sapwood area was determined by locating the maximum and minimum radius on a disk, measuring the total length and sapwood width along those radii, and computing areas of circles from the corresponding radii.

Development of fixed effects, mixed effects, and tree covariate models

For each species, we fitted the two model forms representing the empirical and functional approaches described in the introduction: (i) a segmented polynomial model as described by Gallant and Fuller (1973) (GF model), and, (ii) a functional components model (FC model) comprising three additive components. For each model form we first derived and fitted a fixed effects (FX) base model, and then introduced tree-level random effects in several combinations of one, two or three parameters to produce a mixed effects (MX) model, evaluating alternatives based on Akaike's information criteria (AIC), and -2 log likelihood

values. From the final MX model, the random effects for each tree (BLUPS) were estimated using best linear unbiased prediction. Next we examined additional tree-level covariates as predictors of the BLUPS from the MX model, and introduced those prediction equations into a mixed-effects TX model and refitted all the parameters. Using the TX model to predict the sapwood profile for a new tree (i.e., one not used in the fitting) requires a complex calibration to estimate the empirical BLUPs of the random effects (Nigh 2012). We refitted the TX model without the random effects to construct the TF model, which does not require the calibration. Decisions related to the inclusion of the BLUP prediction equations were made from the TX model where the random effects and covariance structure accounted for within-tree clustering of the data. We checked that the parameter estimates for the terms common to both TF and TX models were at least similar without and with covariance structure, respectively. All models were fit using SAS procedure NLMixed (SAS ver. 9.2) with model variables defined in Table 3. Pearson residuals were plotted against the actual and predicted values, D, relative D, H, C_L, C_A, C_{RT}, and C_R for all models. Box plots of Pearson residuals were also plotted for the categorical variables site location, plots within sites, and four crown classes (open grown to suppressed), but because these did not suggest any major influence, these variables were not considered further. Model terms were included only if they had a significant effect according to a likelihood ratio test. The root mean square error (RMSE) also provided a measure of model comparison.

GF model for pine and hemlock

GF-FX and GF-MX models

The original Gallant-Fuller (1973) segmented polynomial model comprises intercept, linear and quadratic terms. We dropped the intercept term to constrain sapwood to zero at the top of the tree. Early in the analysis we encountered cases where the upper stem polynomial would produce negative estimates of sapwood area and consequently we also removed the linear term. The resulting model was:

$$[1]\quad S_{ij} = (\beta_2 + b_{2j})D_{ij}^2 + (\beta_3 + b_{3j})(D_{ij} - \alpha_1 C_{Lj})^2 I_1 + (\beta_4 + b_{4j})(D_{ij} - \alpha_2 H_j)^2 I_2 + \varepsilon_{ij}$$

where S_{ij} is the sapwood area (cm^2) of disk i from tree j; D is the distance (m) from apex, C_L is the crown length (m); H is the tree height (m); β_2, β_3, β_4, α_1 and α_2 are fixed effects parameters to be estimated; b_2, b_3, b_4, are the random effects; and ε is the residual error.

The upper and lower join points were implemented by the I_1 and I_2 operators, with the upper join point a proportion of crown length C_L and the lower join point a proportion of tree height (H):

where $I_1 = \begin{cases} 1 \text{ when } D \geq \alpha_1 C_L \\ 0 \text{ otherwise} \end{cases}$ and $I_2 = \begin{cases} 1 \text{ when } D \geq \alpha_2 H \\ 0 \text{ otherwise} \end{cases}$

The GF-FX model version is Eq. 1 with the random effects omitted, and the GF-MX model version is Eq. 1 with the random effects included (Source Code S1).

For the GF-MX model, when estimates of the off-diagonal elements were very close to zero, we refitted the model setting those elements to zero and used a likelihood ratio test to evaluate whether the data supported the use of a more parsimonious covariance matrix.

We addressed heteroscedasticity by modeling the residual variance as a power function of the main covariate, *D* (Pinheiro and Bates 2000, p. 206):

[2] $Var(\varepsilon_{ij}) = \sigma^2 |D_{ij}|^{\delta}$

Identification of additional tree covariates for inclusion in the GF-TX and GF-TF models

The GF tree covariates models were developed through linear and nonlinear regression analysis using additional tree crown covariates to predict the BLUPs from the GF-MX model. Component regressions of each random parameter on tree crown covariates were developed, and the substitution of these component regressions resulted in the GF-TX and GF-TF model versions.

Pine

For pine, the correlation between $\beta_2 + b_2$ and $\beta_3 + b_3$ was ρ =-0.98, so $\beta_3 + b_3$ was predicted from $\beta_2 + b_2$. None of the tree-level covariates helped to explain the variation in $\beta_4 + b_4$ so it was left unchanged for pine. The TX and TF models for pine were:

[3] $S = (b_2 + r_0 C_{RD}^{r_1} C_{RT}^{r_2}) D^2 + (b_3 + r_3 r_0 C_{RD}^{r_1} C_{RT}^{r_2})(D - \alpha_1 C_L)^2 I_1 + (b_4 + \beta_4)(D - \alpha_2 H)^2 I_2$

where β_4, α_1 and α_2 are fixed effects parameters and b_2, b_3, b_4, are random effects as in Eq. 1, $r_0 - r_3$ are fixed effects parameters arising from the substitution of the BLUP equations. The GF-TX model version is Eq. 3 refitted with the random effects included, and the GF-TF model version is Eq. 3 with the random effects omitted and refitted.

Hemlock

The tree covariates models for hemlock included component regressions for $\beta_2 + b_2$, $\beta_3 + b_3$, and $\beta_4 + b_4$ from Eq. 1, and substituting these component regressions into Eq. 1 resulted in:

[4] $S = (b_2 + r_4 + r_5(\ln C_A)) D^2 + (b_3 + r_6 + r_7 C_L + r_8 C_{RT})(D - \alpha_1 C_L)^2 I_1 + (b_4 + r_9 H)(D - \alpha_2 H)^2 I_2$

where α_1 and α_2 are fixed effects parameters and b_2, b_3, b_4, are random effects as in Eq. 1, $r_4 - r_9$ are fixed effects parameters arising from the substitution of the BLUP equations. The GF-TX model version is Eq. 3 refitted with the random effects included, and the GF-TF model version is Eq. 3 with the random effects omitted and refitted.

Functional components (FC) model for pine and hemlock

Derivation of FC-FX and FC-MX models

The FC model comprises three overlapping components central to pipe model theory: the area of sapwood at a given height is proportional to the amount of foliage above it. The first component deals with the region within the crown where the amounts of foliage and sapwood area increase with distance from the apex to the crown base (*DIC*); this component is then constant below the crown base. The second component allows for a linear increase or decrease in sapwood area with distance below the crown base (DBC). Finally, the third component allows the possibility of nonlinear sapwood area butt flare, which is not an element of pipe model theory, but which is widely observed. This component is represented as an exponential decay function of relative height (H_R) along the stem, where H_R ranges from 0 at the soil surface to 1 at the tree apex.
The resulting three component equation was:

$$[5]\ S_{ij} = (\tau_0 + t_{0j})DIC_{ij}^{\tau_1} + (\tau_2 + t_{2j})DBC_{ij} + (\tau_3 + t_{3j})e^{\tau_4 H_{Rij}} + \varepsilon_{ij}$$

$$\text{where } DIC = \begin{cases} D \text{ when } D \le \tau_5 C_L \\ \tau_5 C_L \text{ otherwise} \end{cases} \text{ and } DBC = \begin{cases} D - \tau_5 C_L \text{ when } D \ge \tau_5 C_L \\ 0 \text{ otherwise} \end{cases}$$

and where S_{ij} is the sapwood area (cm^2) of disk *i* from tree *j*; *DIC* is the distance (m) from the tree tip within the crown; *DBC* is the of distance below the crown base (m); H_R is the relative height; $\tau_0 - \tau_5$ are fixed effect parameters to be estimated; t_0, t_2, t_3 are random tree-level effects; and ε is the residual error. The inclusion of the τ_5 parameter defines an 'effective crown base' that might be slightly above (τ_5<1) or below (τ_5>1) the observed crown base. The FC-FX model version is Eq. 5 with the random effects omitted, and the FC-MX model version is Eq. 5 with the random effects included, both refitted. We modeled the residual variance for all FC models as described in Eq. 2.

Identification of tree covariates for inclusion in the FC-TX and FC-TF models

The FC tree covariates models were developed through linear and nonlinear regression analysis using additional tree crown covariates to predict the BLUPS from the FC-MX model. Component regressions of each random parameter on tree crown covariates were developed, and the substitution of these component regressions resulted in the FC-TX and FC-TF model versions.

Pine
After substituting the component regressions into Eq. 5, the resulting FC-TX and FC-TF models for pine were:

$$[6]\ S = (t_0 + d_0 \mathrm{C_{RD}} + d_1 H_{CB})DIC^{\tau_1} + (t_2 + d_2 C_{RD} + d_3 H)DBC + (t_3 + d_4 + d_5 C_A C_L)\, e^{\tau_4 H_R}$$

where τ_1, τ_4 and τ_5 are fixed effect parameters to be estimated and t_0, t_2, t_3 are random tree-level effects as in equation 5; d_0 to d_5 are fixed effects parameters arising from the substitution of the BLUP equations. The FC-TX model version is Eq. 6 refitted with the

random effects included, and the FC-TF model version is Eq. 6 with the random effects omitted and refitted.

Hemlock
After substituting the component regressions into Eq. 5, the resulting FC-TX and FC-TF model for hemlock was:

[7]
$$S = (t_0 + d_6 + d_7 lnC_A + d_8 C_{RT}) DIC^{\tau_1} + (t_2 + d_9 + d_{10} lnC_A + d_{11} C_{RT}) DBC + (t_3 + d_{12} lnC_A) e^{\tau_4 H_R}$$

where τ_1, τ_4 and τ_5 are fixed effect parameters to be estimated and t_0, t_2, t_3 are random tree-level effects as in equation 5; d_6 to d_{12} are fixed effects parameters arising from the substitution of the BLUP equations. The FC-TX model version is Eq. 7 refitted with the random effects included, and the FC-TF model version is Eq. 7 with the random effects omitted and refitted.

To examine the influence of tree height and crown ratio on sapwood area, we generated predictions for both species using the GF-TF and FC-TF models with tree height set at the middle of its range in our data, and with crown ratio set at 0.2, 0.5 and 0.8 of its range. We computed crown length from tree height and crown ratio. The remaining TF covariates—crown radius and crown area—were derived from a regression that estimated crown radius from crown length. We also compared the sapwood area profiles between species for trees of the same size using a tree height of 25 m and a crown ratio of 0.5. These data are summarized in the figures of sapwood area against relative distance from apex for both tree species.

Validation data

We predicted sapwood area profile for trees in the pine validation data set using the GF-TF and FC-TF models fitted to the BCMFLNR data. Absolute differences (actual minus predicted) were plotted against basic measures of site, tree (height, crown class, social status) and silvicultural treatment to explore differences between the GF and FC models. Models were also assessed by comparing prediction bias at different points along the stem.

Results

Fixed effects (FX) models

The β_2 values in the GF-FX model indicated that within crown sapwood area increased more rapidly with distance from apex (D) in pine compared to hemlock (Tables 4 and 5). In the GF-FX middle segments, β_2 and β_3 parameters were opposite in sign but almost equal in magnitude in pine; furthermore, since the coefficients of D are additive below the upper join point α_1, the pine middle segment had a roughly linear increase toward the base (Table 4). The larger β_4 parameter for the hemlock GF-FX model indicated greater butt flare compared

to pine (below the lower join point α_2). The α_1 values also indicated that the upper join point occurred much lower in the crown for hemlock than in pine, but the lower join points (α_2 values) were in similar relative positions for the two species.

The upper transition point for pine was much higher in the GF-FX than in the FC-FX model (α_1=0.239 vs. τ_5=0.688, Tables 4 and 6). For hemlock, the estimated transition point locations were slightly lower in the GF-FX compared to the FC-FX models (Tables 5 and 7, α_1 vs. τ_5). The parameter values of both species for the middle component (τ_2) were similar in the FC-FX models, but it was difficult to compare species since the top component is additive to the middle component (Tables 6 and 7). The FC-FX bottom sapwood component was a function of τ_3, τ_4 and tree height, and displayed greater butt flare for hemlock than for pine. In summary for both species, the FC-FX and GF-FX models shared similarities in that the sapwood area in the upper stem was a function of crown length and the butt flare of sapwood area was a function of tree height.

Mixed effect (MX) models

For both pine and hemlock, the best fitting mixed effects models incorporated three random effects (Tables 4-7 variance components), and resulted in substantially improved model fit compared with the FX model. This variation indicates individual-tree differences were not adequately described in the FX models. The butt region had the largest amount of random tree-level variation for both the GF-MX and FC-MX models (b_4 and t_3 parameters, respectively). Tree-level random effects considerably reduced the standard error of the fixed effect population parameters at the butt (β_4, τ_3) compared to the FX model, as expected (Tables 4-7, FX vs. MX). Inclusion of tree-level random effects for mid and upper segments or components affected parameter estimates to a lesser degree than for the butt region. The GF-MX pine parameters for upper and mid sections (β_2 and β_3) still remained opposite in sign and of similar magnitude, predicting the nearly linear but increasing sapwood midsections at the population level, but now allowing the two parameters to vary by tree through b_2 and b_3; consequently, this allowed the possibility of nonlinear increase in sapwood midsections for certain trees. The addition of the random effects did not shift the join or transition point locations in either the GF or FC model, except that the upper transition point was higher in the hemlock FC-MX model (Table 7, τ_5).

Another important aspect of the MX model versions was the variance-covariance structure. The covariances proved to be more important for hemlock, especially between the middle and bottom segments for the FC model compared to the pine (Tables 4-7, Cov). The pine MX models only required covariance between the top and middle segments (Cov b_2, b_3) indicating less dependence between the lower sections (Tables 4 and 6).

Tree covariate mixed effect (TX) models

In all models, the variances and standard errors of the random terms were reduced in the TX models compared to the MX models (Tables 4-7) which substantially improved fits

compared to the FX model, especially the FC-FX model (Fig. 2 and 3). Covariances were similarly reduced in all cases in the TX model compared to the MX model except the pine GF-TX (Table 4).

Tree covariate fixed effect (TF) models

Estimates of the fixed effect parameters were similar between the TX and TF models except for the butt flare sapwood parameter in the GF model (β_4-Table 4). In the GF-TF and FC-TF pine models, sapwood increased with larger crown but more slowly with *DIC* on shorter trees (trees with lower height to crown base or larger crown ratio). In the GF-TF and FC-TF models for hemlock, sapwood area in the upper component decreased with larger crown ratio. For both species, the fit of the top component was always improved by accounting for trees with wider crown or larger crown area, regardless of model form.

Crown variables had varying effects on middle segment or component of both models. In general for both species, crown variables had opposite effects in the midsection compared to the upper section; as a consequence, this allows less rapidly changing but still increasing sapwood area. Further, trees had less sapwood area in the midsections, but this was increased when the crown extended lower proportionately on the tree.

In the butt region, the other components were additive to those controlling this section, but these had a small effect due to the size and configuration of the functions controlling the butt area. The lower component of the FC-TF model declined to 10% of its ground-level sapwood value at a relative height of 0.05 for pine and a relative height of 0.01 for hemlock (from $\ln(0.1)/\tau_4$); consequently, the influence of the lower component was confined to the lowermost portion of the FC tree model. The sapwood area in the pine butt segment of the GF-TF model was associated with greater sapwood area in taller trees. Additionally, the pine FC-TF model showed increased butt sapwood area with crown area and length (d_5-Table 6). For hemlock, the GF-TF model, butt sapwood area increased with tree height (r_9-Table 5) and in the FC-TF model with crown area (d_{12}-Table 7). That is, larger crowns on taller trees were associated with greater sapwood area at the butt.

The join or transition points in all models were largely unchanged by the additional tree-level fixed effect covariates in the TF models compared to the MX.

Comparison of model fit and shape

As expected, the goodness of fit in every case was best in the TX model, followed by the MX, TF, and FX models, respectively (Table 8). The goodness of fit between the MX and TX models was close, and the standard errors of parameters in common to all models were nearly always lowest in the MX or TX model (Tables 4-7). The reduction in RMSE obtained by adding tree-level covariates (TF vs FX) was greater for the FC than for the GF models (Table 8). Over all trees, the model goodness of fit statistics for both species indicated better fit in the FC-TF compared to GF-TF model (Table 8), with the difference mainly resulting from overprediction by the GF model of a few of the larger observations (Fig. 4). Actual

versus predicted values of all trees for pine and hemlock indicated adequate fit (Fig. 4), and residual plots as a function of relative distance from the apex showed similar results (Fig. 5).

Particularly for pine, and to a lesser degree for hemlock, the incorporation of tree-level covariates in the FC-TF model resulted in altered sapwood magnitude and slope compared with the FC-FX model (Fig. 2 and 3-TF vs. FX). For the pine and hemlock GF-TF models, the additional tree-level covariates mainly allowed greater nonlinearity in the sapwood area along the stem compared to the GF-FX model (Fig. 2 and 3). For both pine and hemlock, the FC models had sharper transitions between the top and middle components than for the GF models for all tree sizes (Fig. 2 and 3), which arises from the model specification of its upper transition point. For trees of the same height, pine models tended to predict a slightly more convex shape with moderate and larger crown ratio than in hemlock (Fig. 6). For pine, the GF-TF and FC-TF predicted similar shaped sapwood area across three classes of crown ratio (Fig. 6 top). For hemlock, the GF-TF model predicted that sapwood area was more nonlinear in the mid to lower sections of trees with median or greater crown ratio (Fig. 6 middle). Comparisons between species indicated that the GF and FC models had substantial differences for trees with crown ratio of 0.5; pine displayed greater sapwood area than hemlock above the midpoint of the stem regardless of model form (Fig 6 bottom).

Model validation for pine

We tested the TF predicted values from the models developed for pine against the actual values using a separate validation data set in different locations of BC and Alberta. Overall, the FC model tended to overpredict at large values of sapwood to a greater degree than the GF model (Fig. 7 top). However, the largest differences occurred nearer the tree base, especially for the FC model (Fig. 7 bottom, Table 9) by up to 53% bias. Over all disks, the FC model overpredicted by 9% (observed-predicted) and the GF model underpredicted by 7% for all disks combined, with the largest bias in the butt flare region (Table 9). Parallel results were obtained for the RMSE over all disks which showed the greatest differences at the butt with the GF model having superior prediction (Table 9). Some residual differences were evident in site MK (Alberta), where a few trees in heavily thinned plots had less sapwood area near the tree base than predicted, compared to the unthinned or the lightly thinned plots on that site. Site MK was also one of the least productive of the sites. Site location PS (BC) also had some trees with negative residuals at the tree base, but these occurred in both the thinned and unthinned plots. These residuals were related to trees with smaller sapwood area for their crown length or crown width. However, most of the residuals were clustered around the zero value for all sites and not considered important enough for model inclusion.

Discussion

Model fitting

Our base models fitted to sapwood area along the bole comprised (i) a segmented polynomial model (GF) previously used to describe stem taper, and (ii) a functional components (FC) model derived from pipe model theory. The base fixed effect (FX) models were greatly

improved by introducing tree-level random effects (MX). Some of the tree-level random variation was related to crown variables and tree height, especially near the tree base. Some of the tree-level variation may arise through using simple crown measures as abstractions to the complex three-dimensional distribution of foliage, but we expect this contribution to be small compared to the disk error for the lower stem. Disk-level variation can be increased by sampling error when estimating the sapwood area from disk radii if the sampling strategy does not provide an unbiased estimate when disk shape is not exactly circular. Disks from near the base of the tree are especially prone to sampling error because cross-sections tend to irregular shapes (Cruickshank 2002).

GF vs. FC model

The FC models placed the upper transition point relatively close to the crown base, but the GF models placed this transition higher up. This probably occurs because the polynomial structure of the GF middle component allows this section to describe the increasing sapwood area taper beginning near the base of the crown and into the crown some distance. This frees the upper transition point to float to a higher position near the top where there is a change in sapwood curvature direction. Unlike the FC model, the midsection component of the GF model can accommodate nonlinear taper in the crown section below this point and below the crown. In the FC model, the middle component is essentially linear so the location of the upper transition point must correspond with an abrupt change in modeled taper that occurs near the crown base while also adjusting for mid and lower sections. Both the GF and FC models predicted substantial flare in sapwood area at the base of the trees, which increased with tree height (GF) or also with crown area (FC). The FC model predicted greater curvature in sapwood area at the butt than the GF model, particularly in smaller trees.

Model validation with independent pine data indicated that the GF model predictions had lower bias and RMSE, and mostly, but not completely, due to the differences in the fit in the butt flare region. The GF model polynomial function appears to be more suitable than the FC model exponential decay function for prediction of sapwood area at the base of the validation trees. The validation sites are located further east of the sites used for model building and possibly have regional adaptation in hydraulic function. Both model forms adequately predicted the mid and upper stem sections despite having different bias signs. Model validation revealed positive prediction bias in the GF model, but negative and larger prediction bias in the FC model, either of which could be removed from the predicted values for forestry application. However, the GF model provides lower actual and percentage bias for prediction of sapwood in independent sites, and therefore would be preferred for application. There were also model similarities such as the inclusion of tree height and crown variables, some of which are known to relate to the amount of sapwood, but these are discussed more fully below. Except at the butt flare, we obtained reasonably good prediction estimates of pine sapwood area over large differences in geographic locations using simple measures of height and crown.

Biological interpretation of models

The simple crown and tree variables in the TF and TX models probably act as surrogates for leaf area. Stem sapwood area has been shown to be strongly related to leaf area of the crown in lodgepole pine (Dean and Long 1986) and in eastern hemlock (Kenefic and Seymour 1999). Pipe model theory suggests that the area of stem conductive tissue is equal to the sum of the areas of the smaller branch orders it supplies (Zimmermann 1983 p. 66), so that sapwood area is proportional to the amount of foliage above a point on the stem. Water flow through a stem is related to the product of its conducting area times its water permeability. Consequently, sapwood area should increase from tree apex to the bottom of the crown and then remain constant if the tracheid size, number, and conductivity of the sapwood remain constant along the stem below the crown.

We found that both model types showed a nonlinear increase of sapwood within the crown consistent with leaf area increasing with *DIC*. Pine and hemlock maximum leaf area increased and decreased nonlinearly with relative distance from the apex, with a maximum at 0.33 in pine (Garber and Maguire 2005), and at 0.65 in western hemlock trees of similar size (Kershaw and Maguire 1995). This is consistent with hemlock's higher shade tolerance and greater needle longevity. We found that the sapwood area inflection or transition point in the GF model occurred at 0.25 and 0.63 relative distance into crown for pine and hemlock, respectively, consistent with the vertical distribution of leaf area of these species described above. The same inflections were predicted to occur nearer the crown base for the FC model, less consistent with changes in vertical distribution of leaf area and pipe model theory, for model configuration reasons discussed in the previous section. Further, tree-level parameters such as crown length and width were positively associated with crown sapwood, consistent with pipe model theory, and with expected linkages between vertical foliage distribution and crown size (Kershaw and Maguire 1995). The greater leaf area in the upper pine crown might explain the greater amount of pine sapwood area compared with that from the same location in hemlock of similar size. Nevertheless, other factors might also contribute; for example, greater sapwood area in upper stems might provide water storage needed for growth in drier and warmer habitats in which pine grows.

We found increasing sapwood area below the crown towards the base of the tree in both model forms and tree species, suggesting that tracheid geometry, or conductivity of the sapwood does not remain constant along the stem below the crown. Tracheids become longer and wider with increasing age or stem diameter, from branch to root (top to bottom), and within annual rings from latewood to earlywood (Zimmermann 1983, p. 89). Wider rings are found within the crown region of conifers compared to lower stem positions, except in dominant trees (Farrar 1961); however, we did not find any relationship between model residuals and social status, probably because this was partly reflected in model parameters for tree and crown size. In conifers, the percentage of latewood also decreases with the wider rings (Smith 1980) that are characteristic of the upper stem. Latewood forms first at the base of the tree and then progresses upwards (Young 1952) probably related to the diminishing auxin levels (Larson 1962) resulting in more latewood closer to the tree base because of the time lag. In Douglas-fir, latewood proportion increases from apex to base (Gartner et al. 2004) and latewood has lower conductivity (Domec and Gartner 2002). Increasing latewood proportion towards the base probably increases stem mechanical strength, but results in lower

sapwood conductivity from apex to tree base. This would be a reasonable explanation for the increase in sapwood area toward the lower stem.

It is not clear why the sapwood area greatly increases in the bottom 10% or less of the sample trees (study tree disks start at 0.3 m), but it may satisfy a requirement to maintain water flow locally through this region. We found that the sapwood in this area was most consistently affected by tree height and to a lesser extent by crown variables in all models. Increases in both variables would be associated with increased bending stress at the butt section. Douglas-fir seedlings artificially bent and held in one direction had impaired permeability of the stem in the bent area (Spicer and Gartner 2002). Unlike the seedlings, bending tension and compression in the butt sapwood and extending into the buttressed roots of tall trees would take place in all directions, especially in dominant trees. Trees that were artificially prevented from sway showed higher growth in the area of sway prevention and lower growth below in the butt flare region and buttressed roots, suggesting stem growth is altered by local mechanical bending stress (Fayle 1968). Spruce roots showed decreasing root hydraulic conductivity with larger root system size (Rüdinger et al. 1994) which might be related to structural requirements to accommodate bending stress in the wood needed for taller trees or more frequent tracheid damage in this area. Sapwood tracheids may be affected by mechanical stress or increased cavitation risk especially in older sapwood at the tree base, causing low or nonexistent functionality with age (Spicer and Gartner 2001). It is possible that a tradeoff between conductivity and mechanical requirement in the butt flare and buttressed roots is compensated for by an increase in sapwood area. Supporting this notion is the finding that sapwood area is related to leaf area in the stem, is not related in the butt flare region or in the buttressed roots, but is again related at more distal root positions (Coutts 1987) that are under lower bending stress. Proximal root sections have cells with lower radial and tangential diameter, length, and have thicker cell walls compared to more distal sections (Fayle 1968) which combined would restrict sapwood permeability. The same cell attributes probably extend upward into the stem in addition to the changes in latewood proportion noted above.

Application of sapwood/heartwood estimates to forest management

Remote sensing methods such as small footprint high density laser imaging detection and ranging (LiDAR) systems have potential to estimate individual tree attributes including tree height, and crown height and diameter (Wulder et al. 2008). Sapwood estimates from remote inventory would allow for a complete sapwood inventory of all trees spatially within stands at the planning stage of forest management. Sapwood and heartwood area based on crown or height dimensions of individual trees has practical application for processing raw material in the wood-based industry. When the target is to maximize product sapwood content, the trees can be selected by crown and height through spatial referencing, and bucking and transport operations could take into account this within-piece variation. At the mill level, processing of wood veneer is affected by the difference between sapwood and heartwood moisture content (Huang et al. 2012). Segregating logs based on sapwood could increase the quality and lower cost of the raw materials especially if they can be allocated to product needs, and forecasting and scheduling at the harvesting stage. Sapwood and heartwood also have chemical and physical properties which can guide segregation of raw materials. Heartwood

differs from sapwood in chemical composition (Bertaud and Holmbom 2004) which can affect pulping (Esteves et al. 2005), drying rate (Pang 2000), checking (Lee et al. 2004.), natural durability (Taylor et al. 2002), and uptake of preservatives (Hansmann et al. 2002).

Our models also suggest that sapwood might be manipulated by silvicultural treatments. Lowering stand density increases the amount of sapwood and heartwood in black spruce (Yang and Hazenberg 1992), and increased the area of both sapwood and heartwood as well as the proportion of heartwood in western redcedar (DeBell and Lachenbruch 2009). In contrast, thinning Scots pine increased sapwood area marginally, with little effect on the heartwood area (Mörling and Valinger 1999). Fertilisation increased the amount of leaf area but not sapwood area in Sitka spruce (Whitehead et al. 1984). Clearly more research is needed to sort out the effect of stand manipulation on sapwood and heartwood formation along the stem and to relate this to tree height, crown dimensions, and foliage biomass and distribution.

References

Bamber, R.K., and K. Fukazawa. 1985. Sapwood and Heartwood: a review. *For. Abstr*. 46:567-580.

Bergström, B. 2003. Chemical and structural changes during heartwood formation in *Pinus sylvestris. Forestry* 76:45-53.

Bertaud, F., and B. Holmbom. 2004. Chemical composition of earlywood and latewood in Norway spruce heartwood, sapwood and transition zone wood. *Wood Sci. and Technol.* 38:245-256.

Björklund, L. 1999. Identifying heartwood-rich stems of pinus sylvestris by using inventory data. *Silva Fennica* 33(2):119-129.

Booker, R.E., and J.A. Kininmonth. 1978. Variation in longitudinal permeability of green radiata pine wood. *NZ. J. For. Sci.* 8:295-306.

Coutts, M.P. 1987. Developmental processes in tree root systems. *Can. J. For. Res.* 17:761-767.

Cruickshank, M.G. 2002. Accuracy and precision of measuring cross-sectional area in stem disks of Douglas-fir infected by Armillaria root disease. *Can. J. For. Res.* 32:1542-1547.

Dean, T.J., and J.N. Long. 1986. Variation in sapwood area – leaf area relations within two stands of lodgepole pine. *For. Sci.* 32:749-758.

DeBell, J.D., and B. Lachenbruch. 2009. Heartwood/sapwood variation of western redcedar as influenced by cultural treatments and position in tree. *For. Ecol. Manage.* 258:2026-2032.

Domec, J.C., and B. Gartner. 2002. Age- and position-related changes in hydraulic versus mechanical dysfunction of xylem: inferring the design criteria for Douglas-fir wood structure. *Tree Phys.* 22:91-104.

Esteves, B., J. Gominho, J.C. Rodrigues, I. Miranda, and H. Pereira. 2005. Pulping yield and delignification kinetics of heartwood and sapwood of maritime pine. *J. Wood Chem. Technol.* 25:217-230.

Farrar, J.L. 1961. Longitudinal variation in the thickness of the annual ring. *For. Chron.* 37:373-349.

Farrar, J.L. 1995. *Trees in Canada.* Fitshenry & Whiteside Ltd., Toronto, Canada. 502 p.

Fayle, D.C.F. 1968. Anatomy. P. 71-138 in *Radial growth in tree roots: Distribution, timing, anatomy.* University of Toronto Faculty of Forestry. Tech. Rep. No. 9.

Gallant, A.R., and W.A. Fuller. 1973. Fitting segmented polynomial regression models whose join points have to be estimated. *J. Am. Stat. Assoc.* 68:144-147.

Garber, S.M., and D.A. Maguire. 2005. The response of vertical foliage distribution to spacing and species composition in mixed conifer stands in central Oregon. *For. Ecol. Manage.* 211: 341-355.

Gartner, B.L., R. Moore, and B.A. Gardiner. 2004. Gas in stems: abundance and potential consequences for tree biomechanics. *Tree Phys.* 24:1239-1250.

Gilmore, D.W., R.S. Seymour, and D.A. Maguire. 1996. Foliage – sapwood area relationships for *Abies balsamea* in central Maine, U.S.A. *Can. J. For. Res.* 26:2071-2079.

Hansmann, C., W. Gindl, R. Wimmer, and A. Teischinger. 2002. Permeability of wood - a review Wood Research. *Drev. Vysk.* 47:1-16.

Huang, S., B.J. Wang, J. Lu, Y. Lei, C. Dai, and X. Sun. 2012. Characterising Changbai larch through veneering. Part 2: Effect of diameter at breast height and radial growth. *BioResources* 7:3076-3092.

Kenefic, L.S., and R.S. Seymour. 1999. Leaf area prediction models for Tsuga canadensis. *Can. J. For. Res.* 29:1574-1582.

Kershaw, J.A. Jr., and D.A. Maguire. 1995. Crown structure in western hemlock, Douglas-fir, and grand fir in western Washington: trends in branch-level mass and leaf area. *Can. J. For. Res.* 25: 1897-1912.

Larson, P.R. 1962. Auxin gradients and the regulation of cambial activity. P. 97-117 in *Tree growth*, Kozlowski, T.T. (eds.). Ronald Press, New York.

Lee, N.H., C. Li, J.H. Choi, and U.D. Hwang. 2004. Comparison of moisture distribution along radial direction in a log cross section of heartwood and mixed sapwood and heartwood during radio-frequency/vacuum drying. *J. Wood Sci.* 50:484-489.

Long, J.N., F.W. Smith, and D.R.M. Scott. 1981. The role of Douglas-fir stem sapwood and heartwood in the mechanical and physiological support of crowns and development of stem form. *Can. J. For. Res.* 11:459-464

Maguire, D.A., and J.L.F. Batista. 1996. Sapwood taper models and implied sapwood volume and foliage profiles for coastal Douglas-fir. *Can. J. For. Res.* 26:849-863.

Mansfield, S.D., R. Parish, J.W. Goudie, K.-Y. Kang, and P. Ott. 2007. The effects of crown ratio on the transition from juvenile to mature wood production in lodgepole pine in western Canada. *Can. J. For. Res.* 37:1450-1459.

Mörling, T., and E. Valinger. 1999. Effects of fertilization and thinning on heartwood area, sapwood area and growth in Scots pine. *Scand. J. For. Res.* 14:462-469.

Nemec, A.F.L., R. Parish, and J.W. Goudie. 2012. Modelling number, vertical distribution, and size of live branches on coniferous tree species in British Columbia. *Can. J. For. Res.* 42: 1072–1090.

Nigh, G.D. 2012. Calculating empirical best linear unbiased predictors (EBLUPs) for nonlinear mixed effects models in Excel/Solver. *For. Chron.* 88(3): 340-344.

Ojansuu, R., and M. Maltamo. 1995. Sapwood and heartwood taper in Scots pine stems. *Can. J. For. Res*. 25:1928-1943.

Pang, S. 2000. Drying of sapwood, heartwood and mixed sapwood and heartwood boards of *Pinus radiata*. *Holz. als. Roh.* 58:363-367.

Panshin, A.J., C. de Zeeuw. 1970. *Textbook of wood technology*. Vol. 1. McGraw-Hill, New York. 736 p.

Pinheiro, J.C., and D.M. Bates. 2000. *Mixed-effects models in S and S-Plus*. Springer, New York. 528 p.

Rüdinger, M., S.W. Hallgren, E. Steudle, and E.D. Schulze. 1994. Hydraulic and osmotic properties of spruce roots. *J. Exp. Bot.* 45:1413-142.

Sellin, A. 1994. Sapwood-heartwood proportion related to tree diameter, age, and growth rate in *Picea abies*. *Can. J. For. Res.* 24:1022-1028.

Shelburne, V.B., and R.J. Hedden. 1996. Effect of stem height, dominance class, and site quality on sapwood permeability in loblolly pine, *Pinus taeda* L. *For. Ecol. Manage*. 83:163-169.

Shinozaki, K., K. Yoda, K. Hozumi, and T., Kira. 1964. A quantitative analysis of plant form – the pipe model theory. I. Basic analyses. *Jap. J. of Ecol.* 14:97-105.

Smith, J.H.G. 1980. Influences of spacing on radial growth and percentage latewood of Douglas-fir, western hemlock and western redcedar. *Can. J. For. Res.* 10:169-17.

Spicer, R., and B.L. Gartner. 2001. The effects of cambial age and position within the stem on specific conductivity in Douglas-fir (*Pseudotsuga menziesii*) sapwood. *Trees* 15:222-229.

Spicer, R., and B.L. Gartner. 2002. Compression wood has little impact on the water relations of Douglas-fir (Pseudotsuga menziesii) seedlings despite a large effect on shoot hydraulic properties. *New Phytol.* 154:633-640.

Taylor, A.M., B.L. Gartner, and J.J. Morrell. 2002. Heartwood formation and natural durability – a review. *Wood Fiber Sci.* 34:587-611.

Waring, R.H., P.E. Schroeder, and R. Oren. 1982. Application of pipe model theory to predict canopy leaf area. *Can. J. For. Res.* 12:556-560.

Whitehead, D., W.R.N. Edwards, and P.G. Jarvis. 1984. Conducting sapwood area, foliage area, and permeability in mature trees of *Picea sitchensis* and *Pinus contorta*. *Can. J. For. Res.*14:940–947.

Wulder, M.A., C.W. Bater, N.C. Coops, T. Hilker, and J.C. White. 2008. The role of LIDAR in sustainable forest management. *For. Chron.* 84:807-826.

Yang, K.C., and G. Hazenberg. 1992. Impact of spacings on sapwood and heartwood thickness in *Picea mariana* (Mill.) B.S.P. and *Picea glauca* (Moench.) Voss. *Wood Fiber Sci.* 24(3): 330-336.

Young, H.E. 1952. Differential time of change from earlywood to latewood along the bole of young loblolly pine trees. *J. For.* 50:614-615.

Zimmermann, M.H. 1983. *Xylem structure and the ascent of sap*. Springer-Verlag, Berlin. 143 p.

List of Supplementary Materials

Supplement 1. SAS NLmixed code to configure the GF-MX model for hemlock.

List of figure captions

Fig. 1 Map of study site locations in British Columbia (BC) and Alberta (AB). Squares represent the hemlock sites, and triangles the pine sites.

Fig. 2 Pine FC and GF model fits showing the sapwood profile along the stem from the apex for the trees of median RMSE in three height classes.

Fig. 3 Hemlock GF model fits showing the sapwood profile along the stem from the apex for the trees of median RMSE in three height classes.

Fig. 4 FC model (left) and GF model observed data versus predicted tree-level covariates model (TF) fitted to the BCMFLNR pine and data.

Fig. 5 Pearson residuals versus relative tree height (0=top) for fixed effects models with tree-level covariates model (TF) fitted to the BCMFLNR pine (top) and hemlock data (bottom). The FC model is on the left and the GF model on the right. The horizontal solid black line represents the model prediction, and the gray horizontal line represents a LOESS curve fitted to the residuals.

Fig. 6 Graph of predicted sapwood area versus relative distance from tree apex (0=top) for pine (top) and hemlock (middle) fit with the tree-level covariates model (TF). The GF and FC model versions are shown in each panel for each species. The top two panels show the effect of crown ratio at 20th, 50th and 80th percentiles of the range for trees at the 50th height percentile. The bottom panel compares the sapwood distributions for trees with height 25 m tall and a crown ratio of 0.5 for both species and model type.

Fig. 7 Top panel depicts the FC model (left) and GF model for the validation pine observed versus predicted sapwood area. The bottom panel shows differences in sapwood area for the FC model (left) and GF model between the predicted (TF model) and the observed validation pine data versus relative height (0=apex). Grey lines are Loess curve fits.

1 Table 1 Summary of sample tree characteristics.

Data source	Species	# Trees		Disks per tree	Height (m)	dbh (cm)	Crown radius (m)	Crown length (m)	Height base live crown (m)	Sapwood area (cm2)	Disk area (cm2)
Model build	Pl	60	Min.	7	6.2	4.4	0.4	3.9	0.4	1.5	1.5
			Mean	11	19.8	23.0	1.5	8.8	11.0	173.3	281.8
			Max	17	29.2	46.1	3.3	17.9	20.8	1143.0	2256.4
	Hw	124	Min.	7	6.9	4.6	0.7	3.7	0.4	0.0	0.0
			Mean	10	21.0	23.5	2.2	11.8	9.2	288.6	344.7
			Max	13	45.1	64.6	5.5	27.5	29.8	2850.4	3717.6
Validation	Pl	105	Min.	5	12.9	6.9	0.4	1.9	6.0	7.2	8.1
			Mean	6	19.2	18.0	1.2	5.3	13.6	95.4	151.9
			Max	7	28.2	30.4	2.4	10.5	22.9	401.8	705.6

2
3
4
5

Table 2 Summary of sample characteristics for trees in sample plots.

Data source	Species	# sites		Stand basal area (m^2/ ha)	Mean height (m)	Mean dbh (cm)	Site index (m 50 yr)
Model build	Pl	2	Min	5.8	2.6	4.6	13.5
			Mean	36.8	15.4	17.3	20.5
			Max	77.2	26.0	32.7	26.9
	Hw	3	Min	10.6	8.0	7.2	21.4
			Mean	57.7	23.1	24.1	35.4
			Max	121.5	43.1	55.5	46.4
Validation	Pl	6	Min	25.8	8.9	7.6	15.8
			Mean	38.7	16.0	16.2	17.4
			Max	58.1	20.4	26.4	20.0

Table 3 Variable definitions and abbreviations

Variable	Definition
C_A	Crown area (m^2)
C_L	Crown length (m)
C_{RD}	Crown radius (m)
C_{RT}	Crown ratio
D	Distance from apex (m)
H	Tree height (m)
H_R	Relative tree height
H_{CB}	Height to crown base (m)
S	Sapwood area (cm^2)

Table 4 Parameter estimates for the GF models fitted to the BCMFLNR pine data.

Model Parameter	FX		MX		TF		TX	
	Estimate	Std. Error	Estimate	Std. Error	Estimate	Std. Error	Estimate	Std. Error
β_2	4.39	0.23	4.32	0.22				
β_3	-4.69	0.21	-4.75	0.24				
β_4	46.29	44.15	26.09	5.32	6.65	4.56	17.13	5.34
α_1	0.24	0.02	0.26	0.01	0.25	0.01	0.26	0.01
α_2	0.93	0.03	0.90	0.01	0.83	0.05	0.88	0.02
r_0					1.98	0.10	1.91	0.18
r_1					0.67	0.03	0.71	0.07
r_2					-0.60	0.04	-0.65	0.07
r_3					-1.10	0.01	-1.10	0.01
Var (b_2)			1.95	0.41			0.75	0.16
Var (b_3)			2.44	0.53			0.00	0.00
Var (b_4)			252.33	121.36			153.42	100.46
Cov (b_2,b_3)			-2.14	0.46			0.00	0.00
Cov (b_2,b_4)			0.00	0.00			6.51	0.28
Cov (b_3,b_4)			0.00	0.00			0.00	0.00
σ^2	10.51	1.79	9.75	2.03	4.87	0.82	13.67	2.61
δ	2.34	0.07	1.48	0.09	2.42	0.07	1.49	0.08
Degrees Freedom	707		57		707		58	

Table 5 Parameter estimates for the GF models fitted to the BCMFLNR hemlock data.

Model Parameter	FX		MX		TF		TX	
	Estimate	Std. Error	Estimate	Std. Error	Estimate	Std. Error	Estimate	Std. Error
β_2	1.62	0.03	1.64	0.05				
β_3	-2.14	0.08	-1.40	0.13				
β_4	67.07	39.63	62.58	14.09				
α_1	0.68	0.02	0.57	0.01	0.63	0.03	0.55	0.01
α_2	0.92	0.02	0.94	0.00	0.93	0.02	0.94	0.00
r_4					0.47	0.05	0.35	0.14
r_5					0.41	0.02	0.49	0.05
r_6					-1.06	0.14	-1.89	0.31
r_7					-0.15	0.01	-0.12	0.02
r_8					2.26	0.28	3.29	0.33
r_9					2.66	1.52	2.85	0.52
$Var(b_2)$			0.29	0.04			0.18	0.02
$Var(b_3)$			1.52	0.25			0.55	0.11
$Var(b_4)$			4064.00	1496.00			3091.00	1215.00
$Cov(b_2,b_3)$			-0.42	0.08			-0.21	0.04
$Cov(b_2,b_4)$			18.04	5.74			6.09	3.70
$Cov(b_3,b_4)$			-48.81	14.39			-16.38	7.28
σ^2	1.18	0.15	0.82	0.10	0.58	0.07	0.77	0.09
δ	3.26	0.05	2.61	0.05	3.42	0.05	2.64	0.05
Degrees Freedom	1325.00		121.00		1325.00		121.00	

Table 6 Parameter estimates for the FC models fitted to the BCMFLNR pine data.

Model Parameter	FX		MX		TF		TX	
	Estimate	Std. Error	Estimate	Std. Error	Estimate	Std. Error	Estimate	Std. Error
τ_0	3.47	0.27	5.94	0.39				
τ_1	1.94	0.05	1.59	0.03	1.53	0.03	1.57	0.03
τ_2	8.36	0.59	10.99	0.98				
τ_3	345.96	222.26	124.35	28.95				
τ_4	-98.74	42.60	-56.77	9.46	-49.89	16.58	-57.82	9.61
τ_5	0.69	0.02	0.67	0.01	0.70	0.02	0.67	0.01
Var (t_0)			5.19	1.12			1.16	0.27
Var (t_2)			51.35	10.43			16.69	3.79
Var (t_3)			19155.00	6487.00			16918.00	6026.22
Cov (t_0,t_2)			6.49	2.33			0.04	0.64
Cov (t_0,t_3)			0.00	0.00			0.00	0.00
Cov (t_2,t_3)			0.00	0.00			0.00	0.00
d_0					2.67	0.16	2.52	0.22
d_1					0.20	0.01	0.21	0.02
d_2					11.01	0.71	11.51	1.07
d_3					-0.32	0.05	-0.34	0.08
d_4					93.39	40.51	80.98	32.35
d_5					0.40	0.22	0.48	0.22
σ^2	13.39	2.29	7.98	1.60	6.21	1.00	7.63	1.50
δ	2.29	0.07	1.56	0.09	2.18	0.07	1.58	0.09
Degrees Freedom	707		57		707		57	

Table 7 Parameter estimates for the FC models fitted to the BCMFLNR hemlock data.

Model Parameter	FX		MX		TF		TX	
	Estimate	Std. Error	Estimate	Std. Error	Estimate	Std. Error	Estimate	Std. Error
τ_0	0.78	0.04	0.77	0.03				
τ_1	2.38	0.02	2.44	0.02	2.32	0.03	2.43	0.02
τ_2	10.35	0.82	22.75	1.04				
τ_3	1939.82	463.02	890.59	211.29				
τ_4	-159.14	16.04	-165.65	14.58	-176.33	29.50	-165.61	14.25
τ_5	0.84	0.01	0.50	0.01	0.60	0.02	0.50	0.01
Var (t_0)			0.07	0.01			0.05	0.01
Var (t_2)			131.82	17.19			58.51	7.83
Var (t_3)			660736.00	261954.00			498660.00	209633.00
Cov (t_0,t_2)			1.11	0.30			0.47	0.16
Cov (t_0,t_3)			84.44	33.46			0.00	
Cov (t_2,t_3)			3277.28	1361.19			0.00	
d_6					0.75	0.07	0.77	0.12
d_7					0.16	0.02	0.13	0.03
d_8					-0.39	0.07	-0.53	0.12
d_9					-17.31	1.58	-19.31	4.05
d_{10}					10.51	0.42	11.88	0.98
d_{11}					18.79	2.09	16.73	3.98
d_{12}					448.27	161.58	355.53	71.38
σ^2	0.39	0.05	0.05	0.01	0.27	0.04	0.05	0.01
δ	3.70	0.06	3.65	0.06	3.69	0.06	3.65	0.06
Degrees Freedom	1325		121		1325		121	

Table 8 Goodness of fit statistics for the fixed (FX), mixed (MX) and tree level covariates (TF) models for the FC and GF models fitted to the BCMFLNR pine and hemlock data.

Description	FX		MX		TF		TX	
	FC	GF	FC	GF	FC	GF	FC	GF
1) Lodgepole pine								
AIC	7457	7363	6456	6414	6746	6955	6320	6335
RMSE	78.5	72.3	18.7	18.4	47.0	57.2	19.0	18.6
2) Western hemlock								
AIC	13728	13851	11713	12304	13236	13413	11580	12159
RMSE	148.5	131.1	46.8	38.3	118.2	126.8	46.6	38.8

Table 9 Pine validation data set bias (actual - predicted) versus relative height (0=base) and RMSE for the FC-TF and GF-TF models.

Relative height from base	# disks	Bias cm^2				% Bias				RMSE	
		FC	Std. Error	GF	Std. Error	FC	Std. Error	GF	Std. Error	FC	GF
0.05	209	-33.5	4.6	13.3	4.3	53.1	3.6	10.8	3.0	74.7	63.2
0.15	1	-31.2	-	8.1	-	31.2	-	17.4	-	31.2	8.1
0.25	17	-9.7	9.7	7.4	10.7	30.4	6.5	18.3	12.9	40.1	43.6
0.35	91	-9.5	5.0	7.5	4.7	37.6	3.2	8.4	4.1	48.6	45.3
0.45	9	2.6	7.7	3.7	6.0	16.5	5.1	5.5	10.0	22.0	17.5
0.55	103	2.6	3.4	3.8	3.5	27.5	2.0	4.9	3.6	34.2	35.4
0.65	38	-0.4	3.8	2.6	3.9	17.0	2.6	3.7	4.8	23.1	24.0
0.75	105	-0.5	1.8	2.8	1.8	13.9	1.2	5.8	3.0	18.8	18.1
0.85	118	-1.5	1.0	0.9	1.0	7.9	0.7	2.7	3.2	10.7	10.8
0.95	5	1.2	5.7	1.4	5.9	8.7	3.7	1.7	26.6	11.4	11.8
All disks	696	-11.5	1.8	6.5	1.6	9.0	1.6	7.1	1.5	48.1	42.5

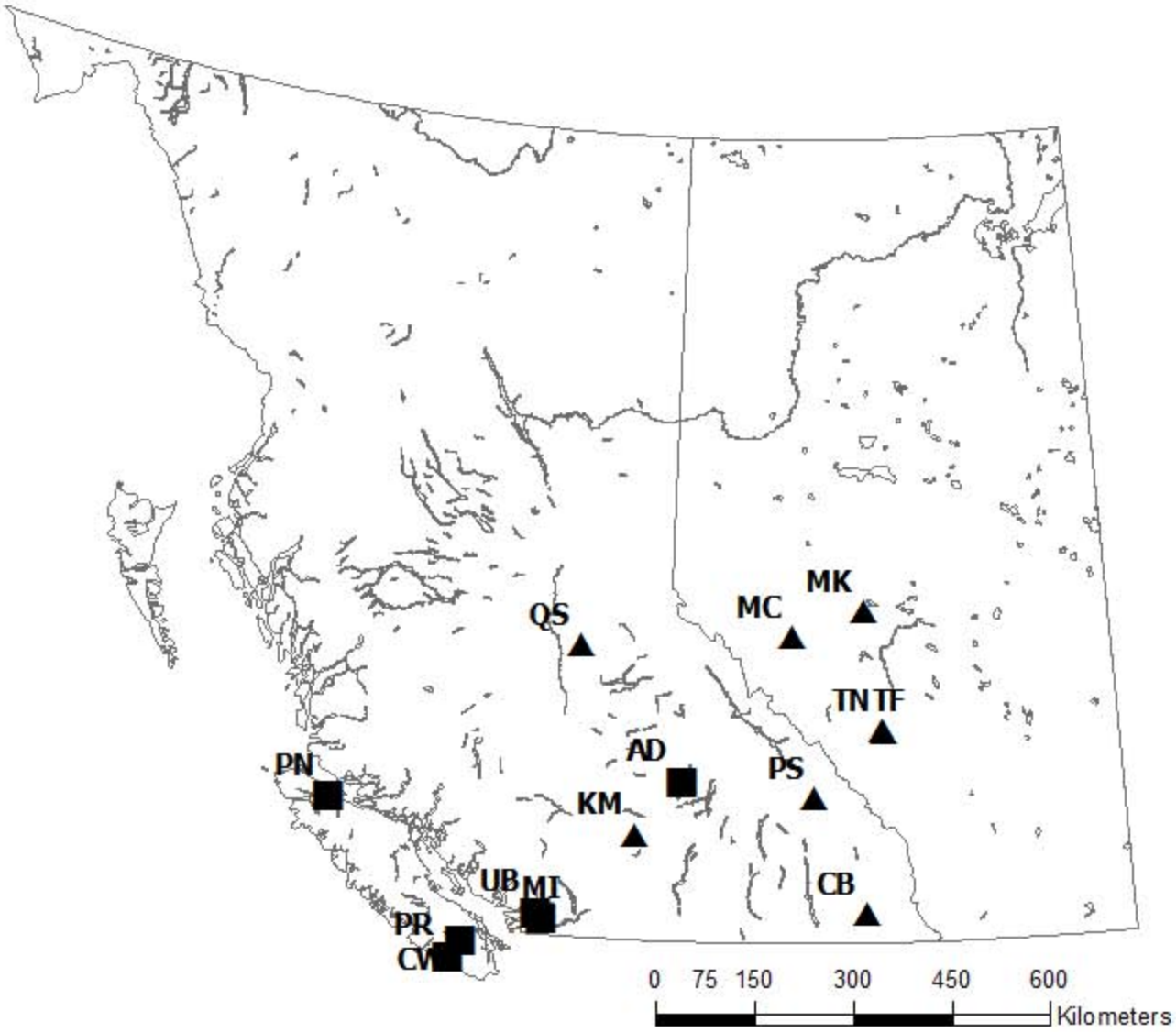
MK
MC
QS
TN
TF
AD
PS
PN
KM
UB
MT
CB
PR
CV
0 75 150 300 450 600
Kilometers

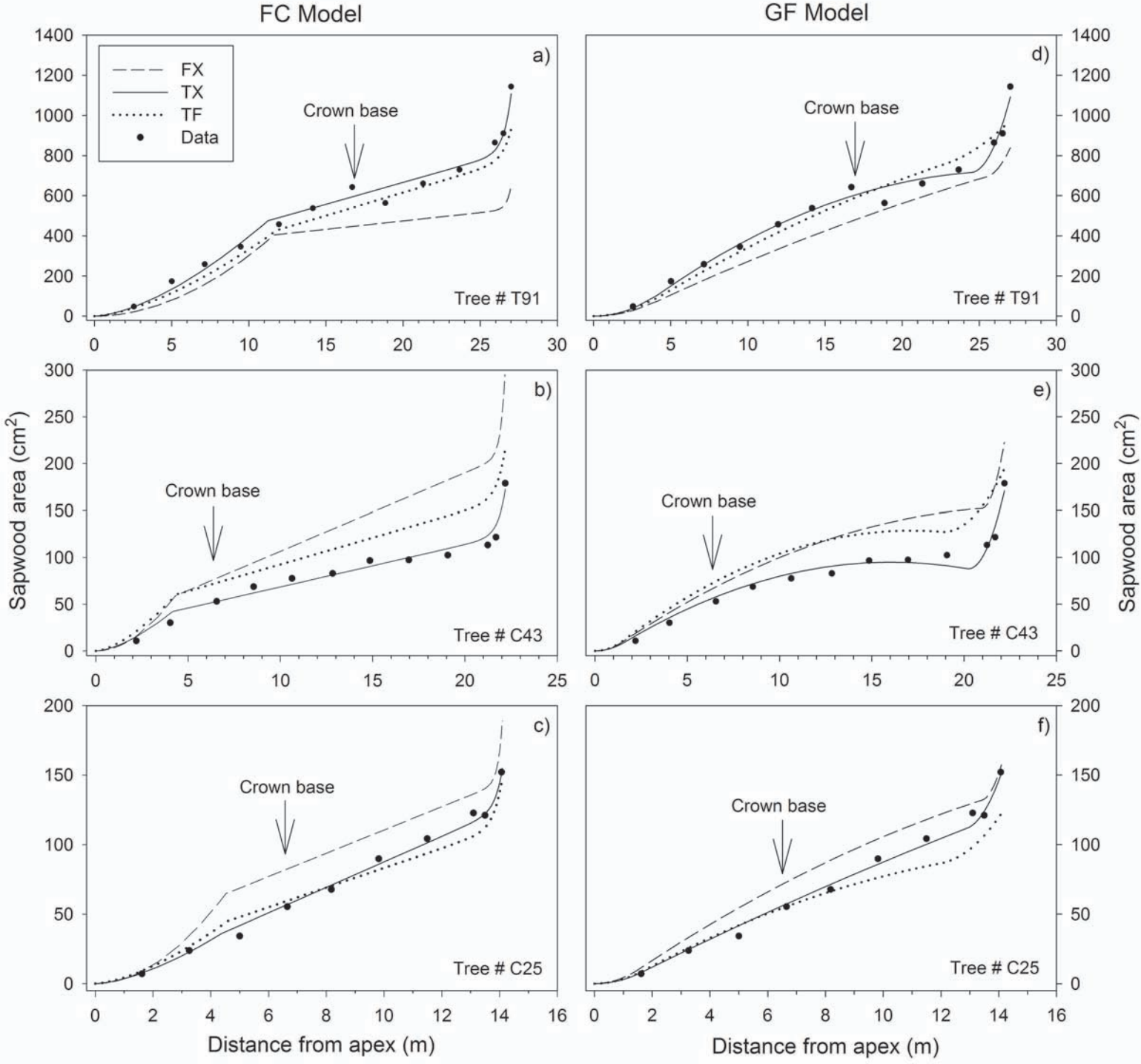
FC Model
GF Model
FX
TX
TF
Data
a)
b)
c)
d)
e)
f)
Crown base
Tree # T91
Tree # C43
Tree # C25
Sapwood area (cm2)
Distance from apex (m)

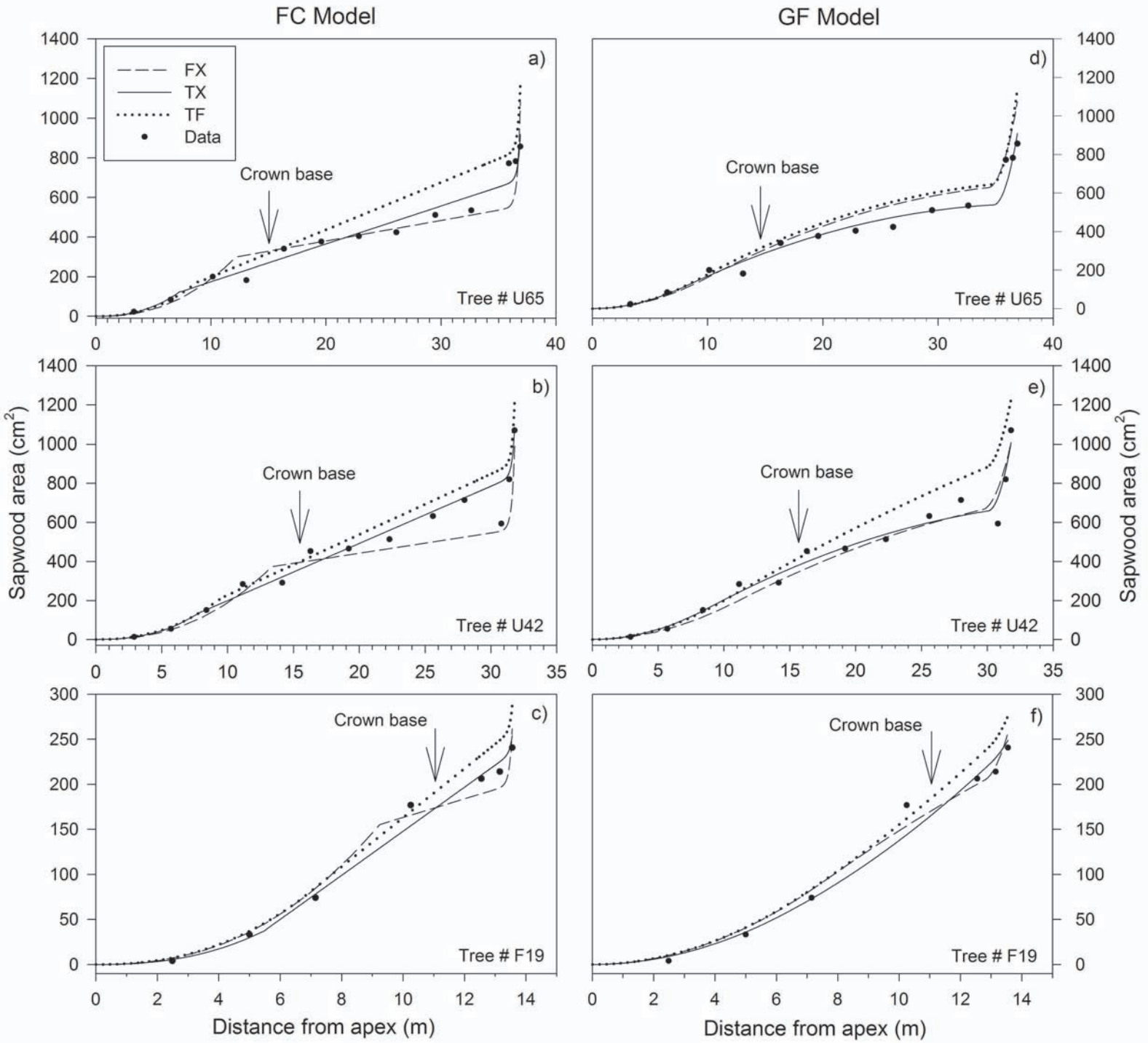
FC Model
GF Model
FX
TX
TF
Data
a)
b)
c)
d)
e)
f)
Crown base
Tree # U65
Tree # U42
Tree # F19
Sapwood area (cm^2)
Distance from apex (m)

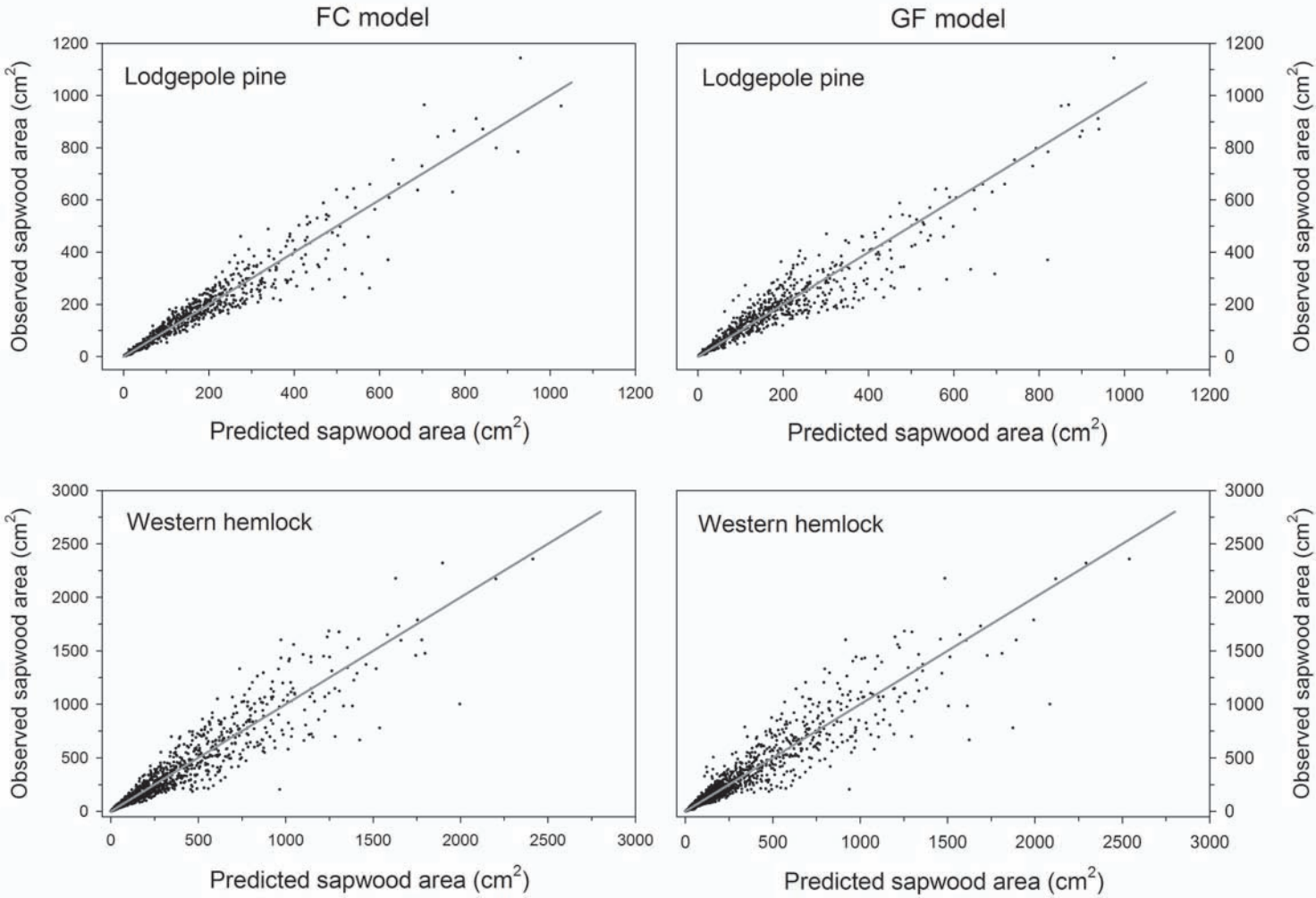
FC model
GF model
Lodgepole pine
Lodgepole pine
Western hemlock
Western hemlock
Observed sapwood area (cm2)
Predicted sapwood area (cm2)
0
200
400
600
800
1000
1200
500
1500
2000
2500
3000

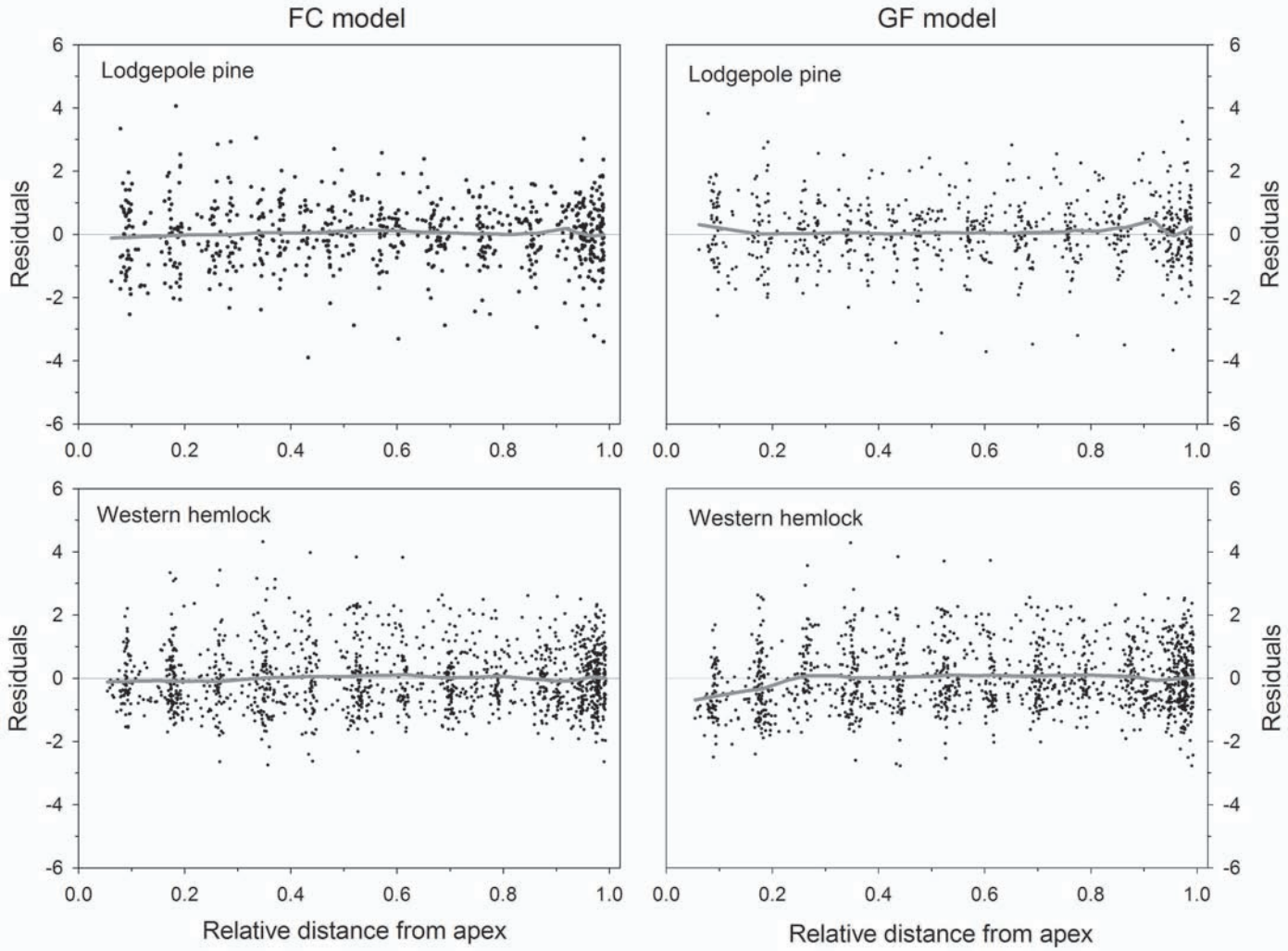
FC model
GF model
Lodgepole pine
Lodgepole pine
Western hemlock
Western hemlock
Residuals
Residuals
Residuals
Residuals
6
4
2
0
-2
-4
-6
0.0
0.2
0.4
0.6
0.8
1.0
Relative distance from apex
Relative distance from apex

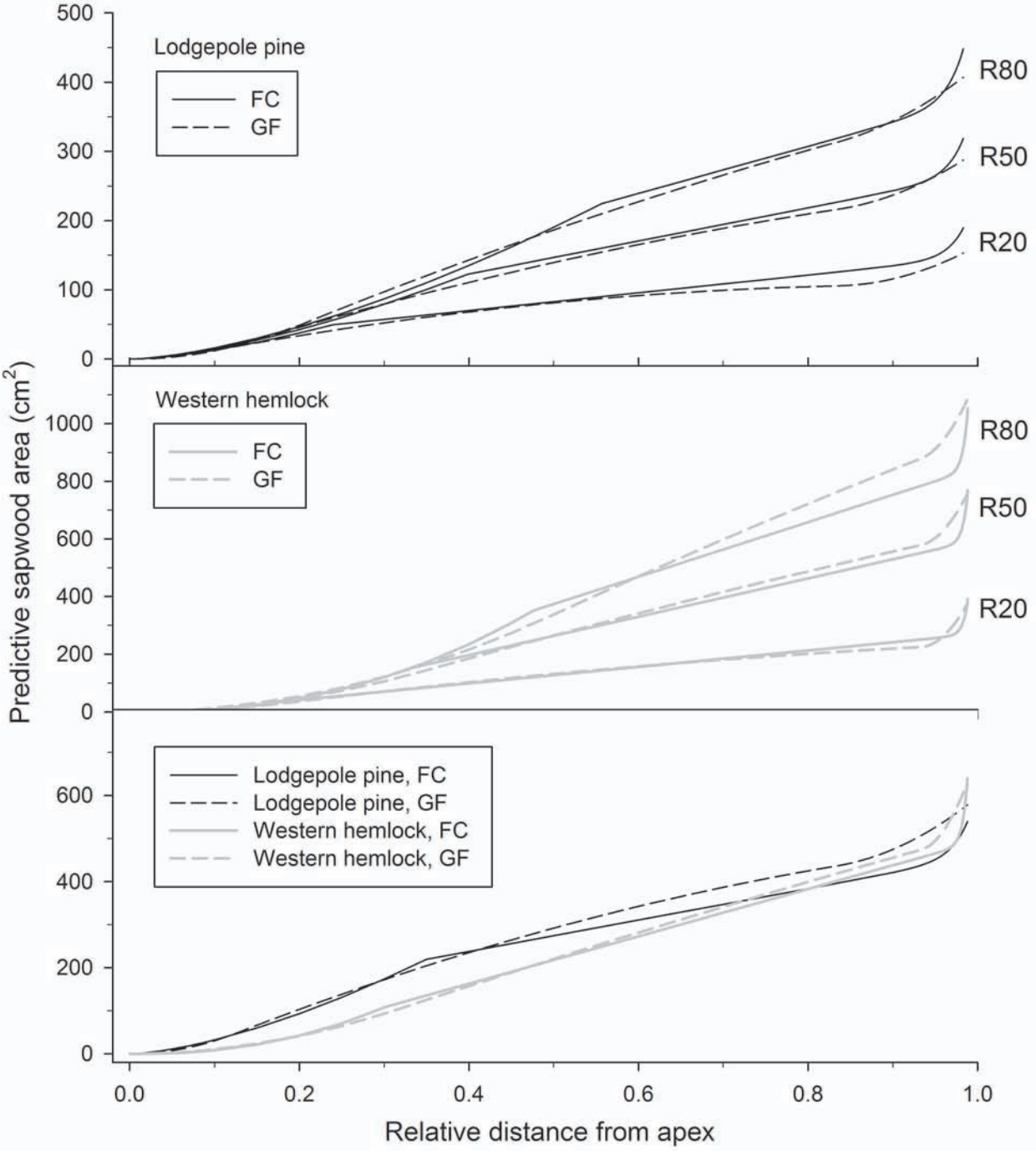
Lodgepole pine
FC
GF
R80
R50
R20
Western hemlock
FC
GF
R80
R50
R20
Lodgepole pine, FC
Lodgepole pine, GF
Western hemlock, FC
Western hemlock, GF
Predictive sapwood area (cm2)
Relative distance from apex
0
100
200
300
400
500
600
800
1000
0.0
0.2
0.4
0.6
0.8
1.0

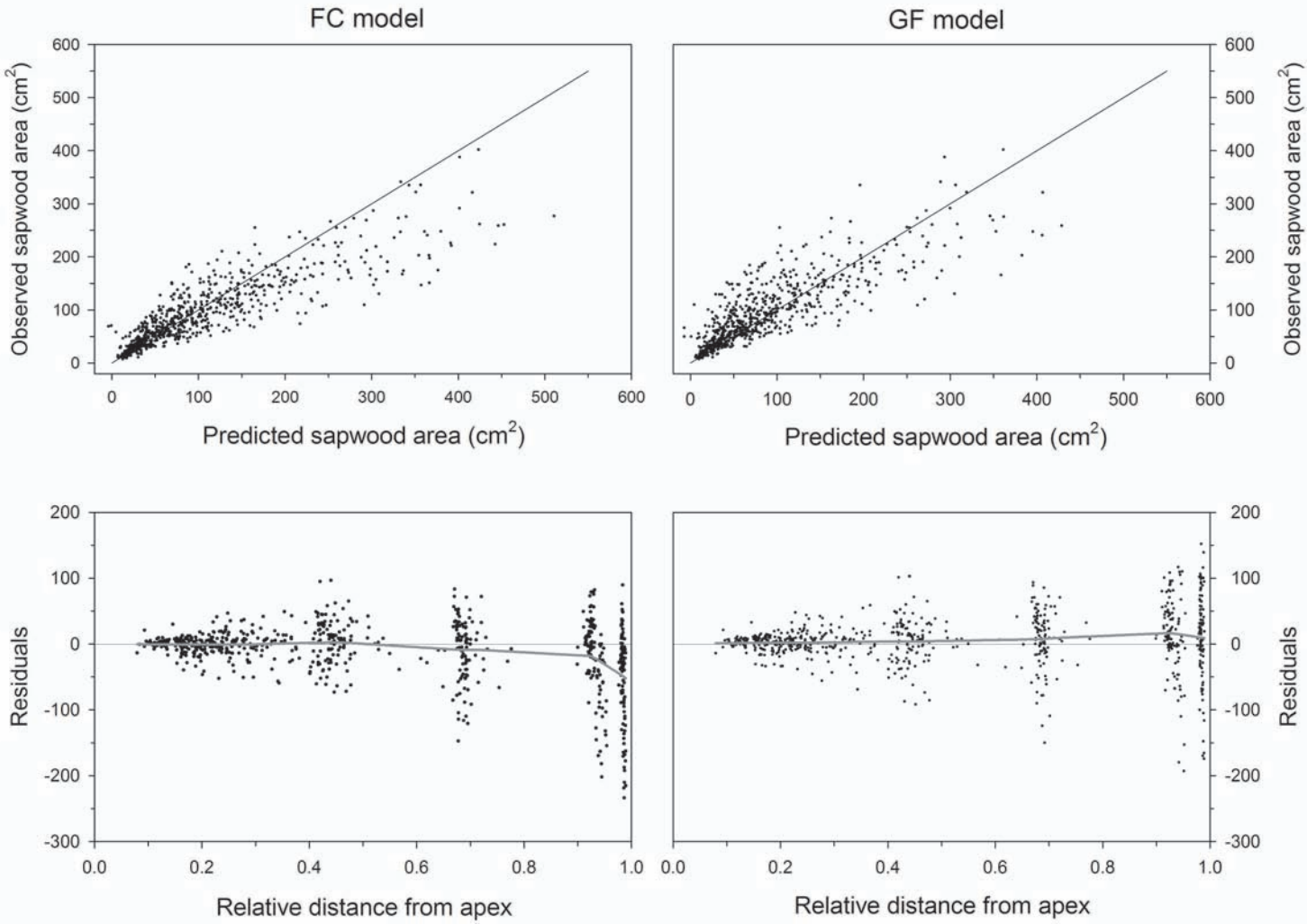
FC model
GF model
Observed sapwood area (cm^2)
Predicted sapwood area (cm^2)
Residuals
Relative distance from apex
0
100
200
300
400
500
600
-300
-200
-100
0.0
0.2
0.4
0.6
0.8
1.0

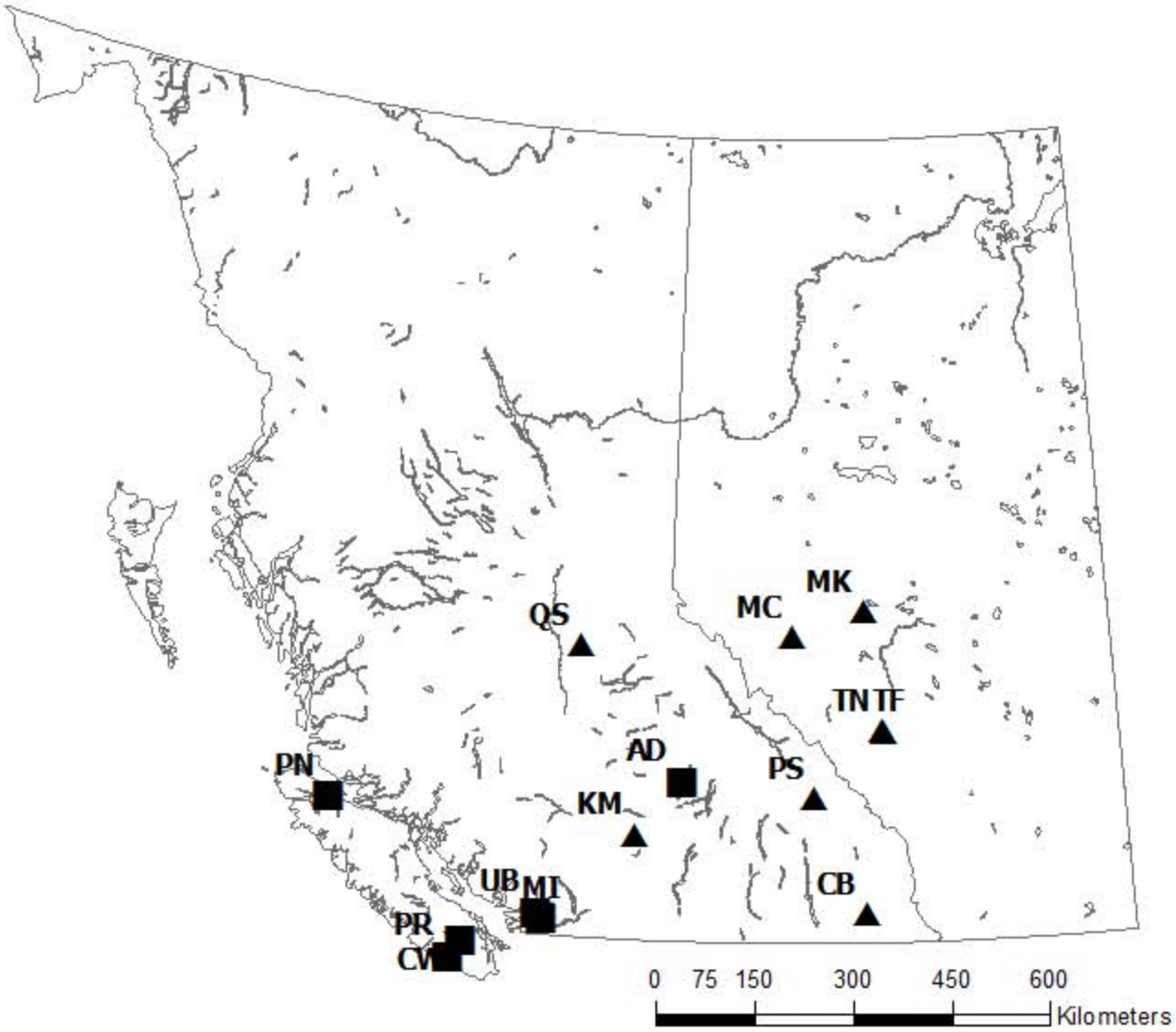
MK
MC
QS
TN
TF
AD
PS
PN
KM
UB
MT
CB
PR
CV
0 75 150 300 450 600
Kilometers

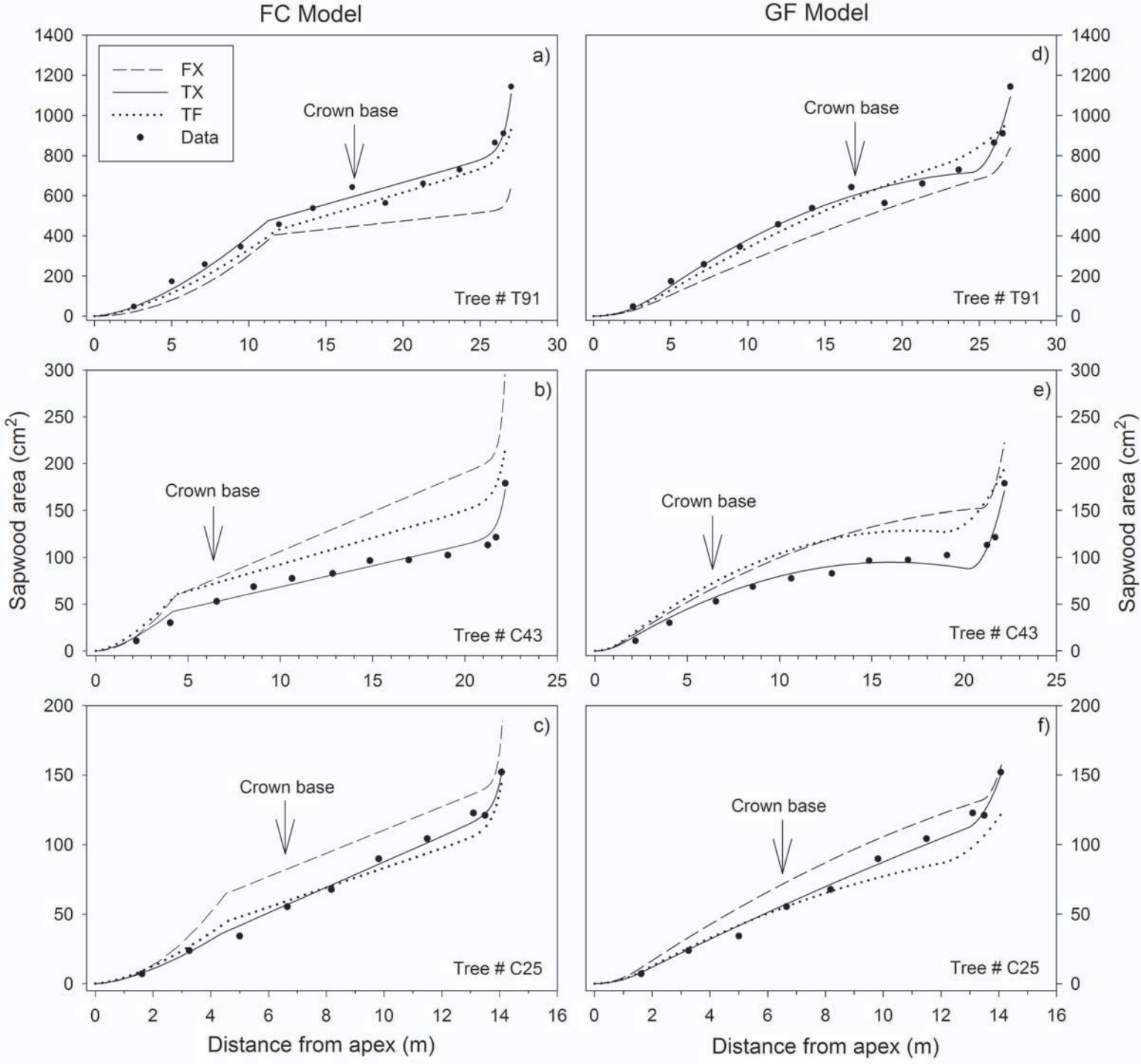
FC Model
GF Model
FX
TX
TF
Data
a)
b)
c)
d)
e)
f)
Crown base
Tree # T91
Tree # C43
Tree # C25
Sapwood area (cm2)
Distance from apex (m)

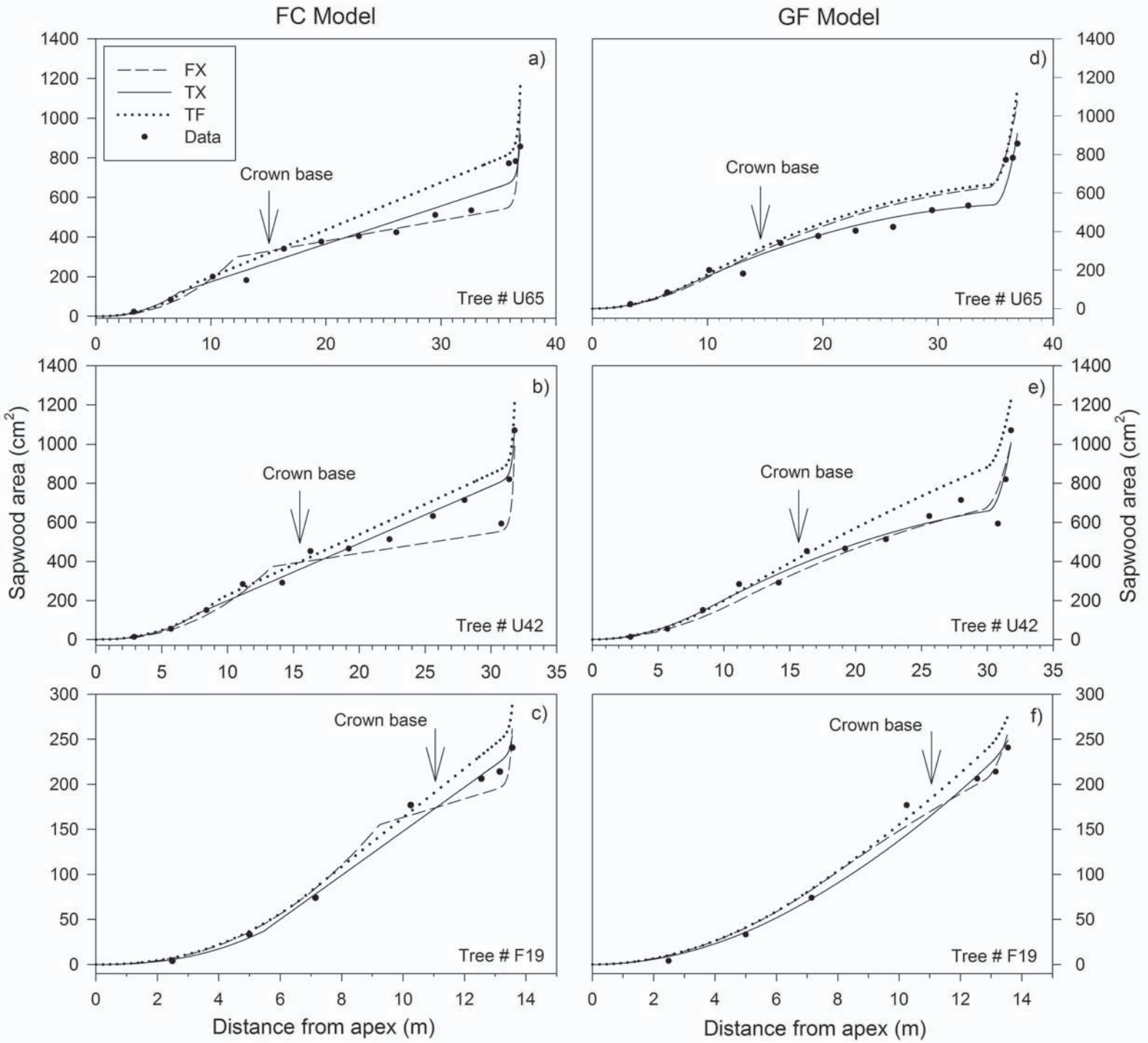
FC Model
GF Model
FX
TX
TF
Data
a)
b)
c)
d)
e)
f)
Crown base
Tree # U65
Tree # U42
Tree # F19
Sapwood area (cm^2)
Distance from apex (m)

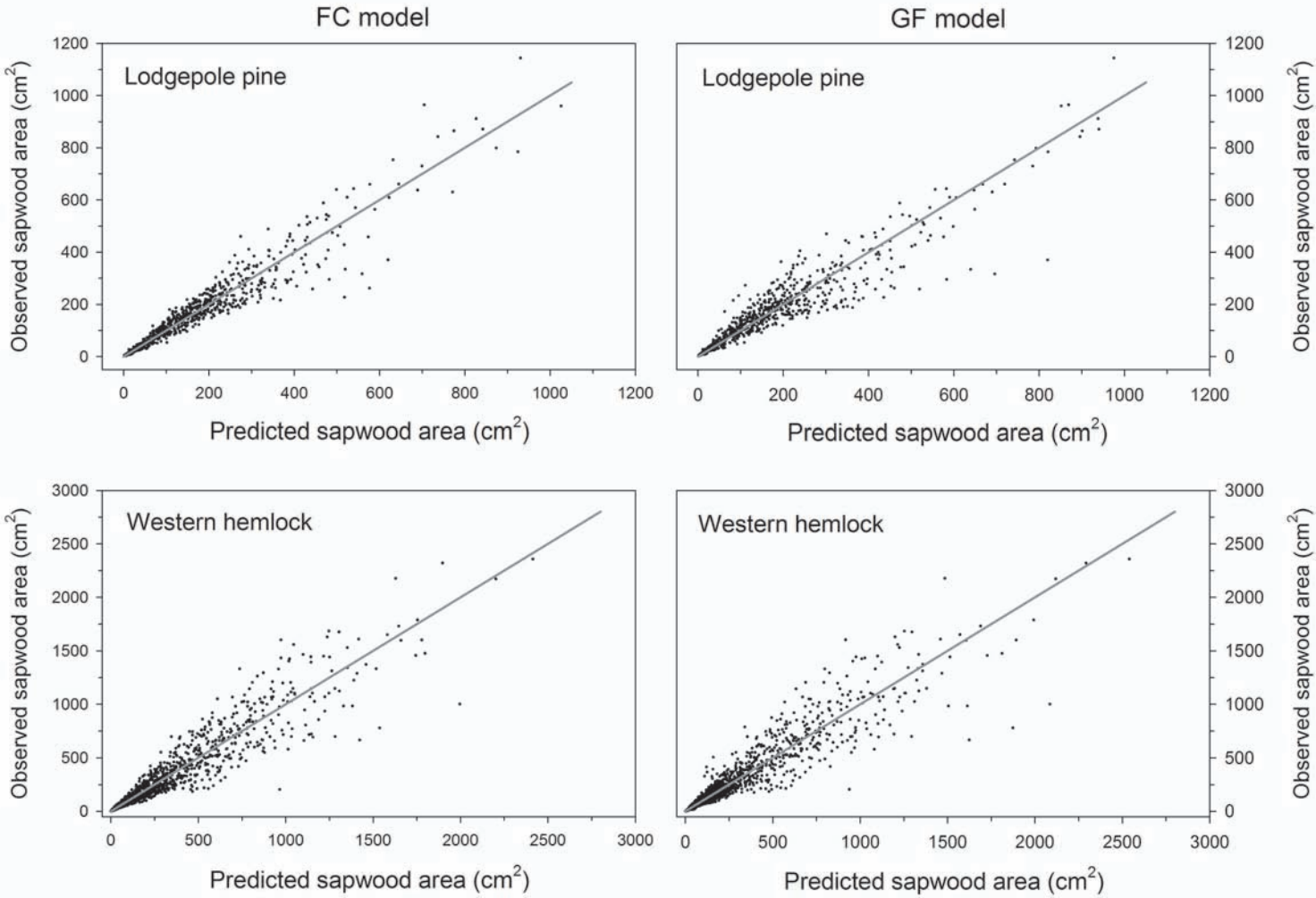
FC model
GF model
Lodgepole pine
Lodgepole pine
Western hemlock
Western hemlock
Observed sapwood area (cm2)
Predicted sapwood area (cm2)
0
200
400
600
800
1000
1200
500
1500
2000
2500
3000

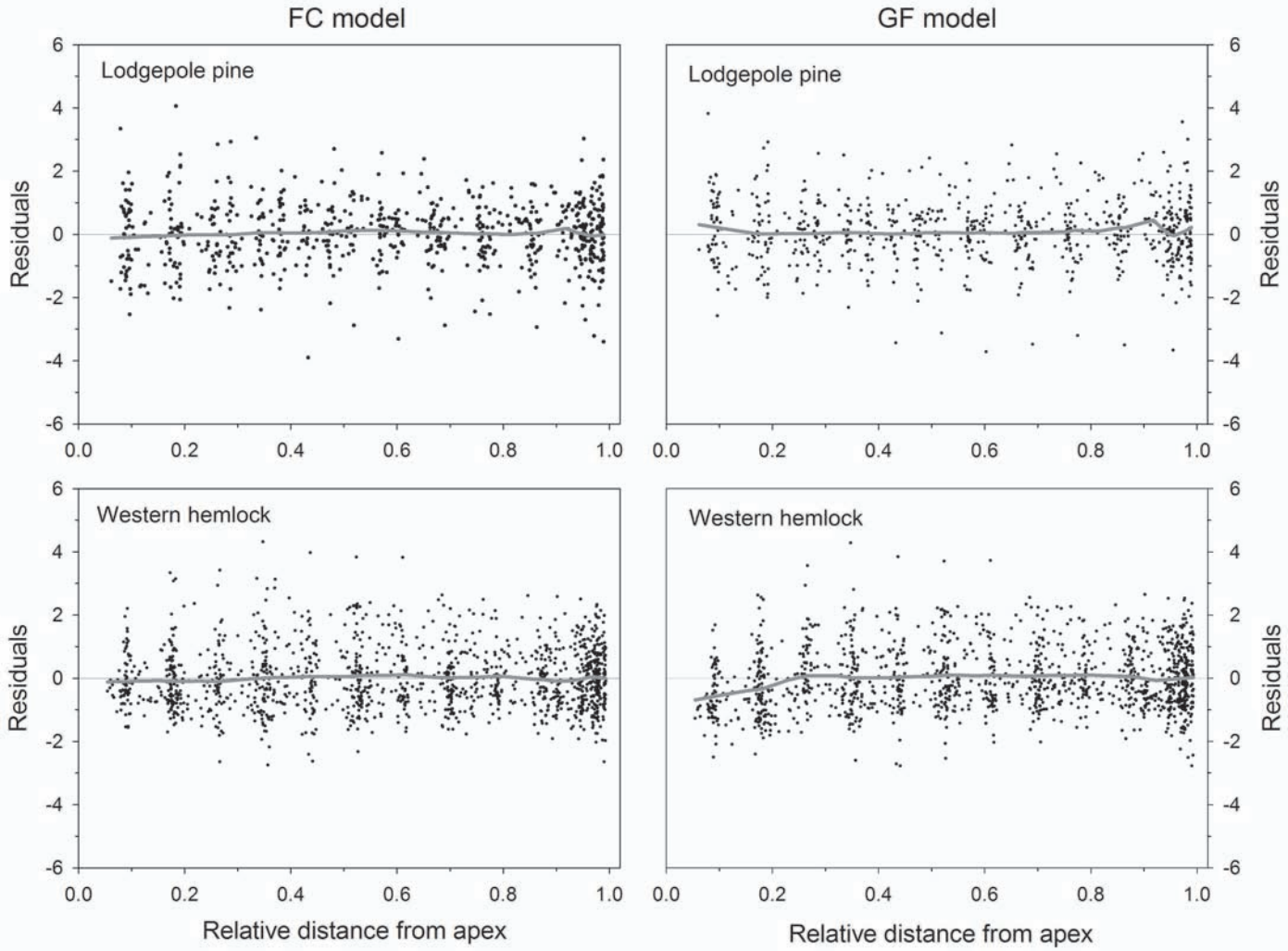
FC model
GF model
Lodgepole pine
Lodgepole pine
Western hemlock
Western hemlock
Residuals
Residuals
Residuals
Residuals
6
4
2
0
-2
-4
-6
0.0
0.2
0.4
0.6
0.8
1.0
Relative distance from apex
Relative distance from apex

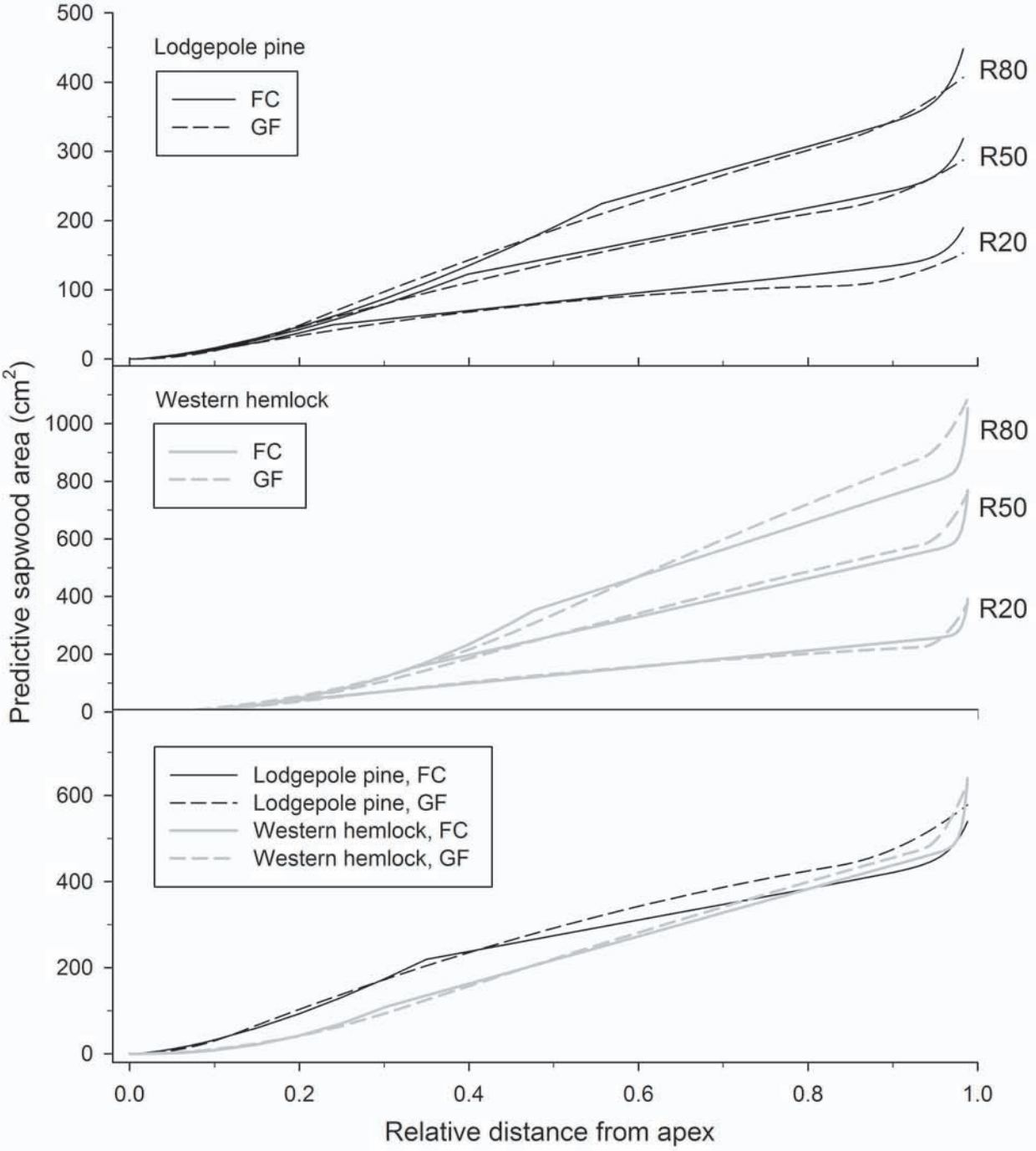
Lodgepole pine
FC
GF
R80
R50
R20
Western hemlock
FC
GF
R80
R50
R20
Lodgepole pine, FC
Lodgepole pine, GF
Western hemlock, FC
Western hemlock, GF
Predictive sapwood area (cm2)
Relative distance from apex
0
100
200
300
400
500
600
800
1000
0.0
0.2
0.4
0.6
0.8
1.0

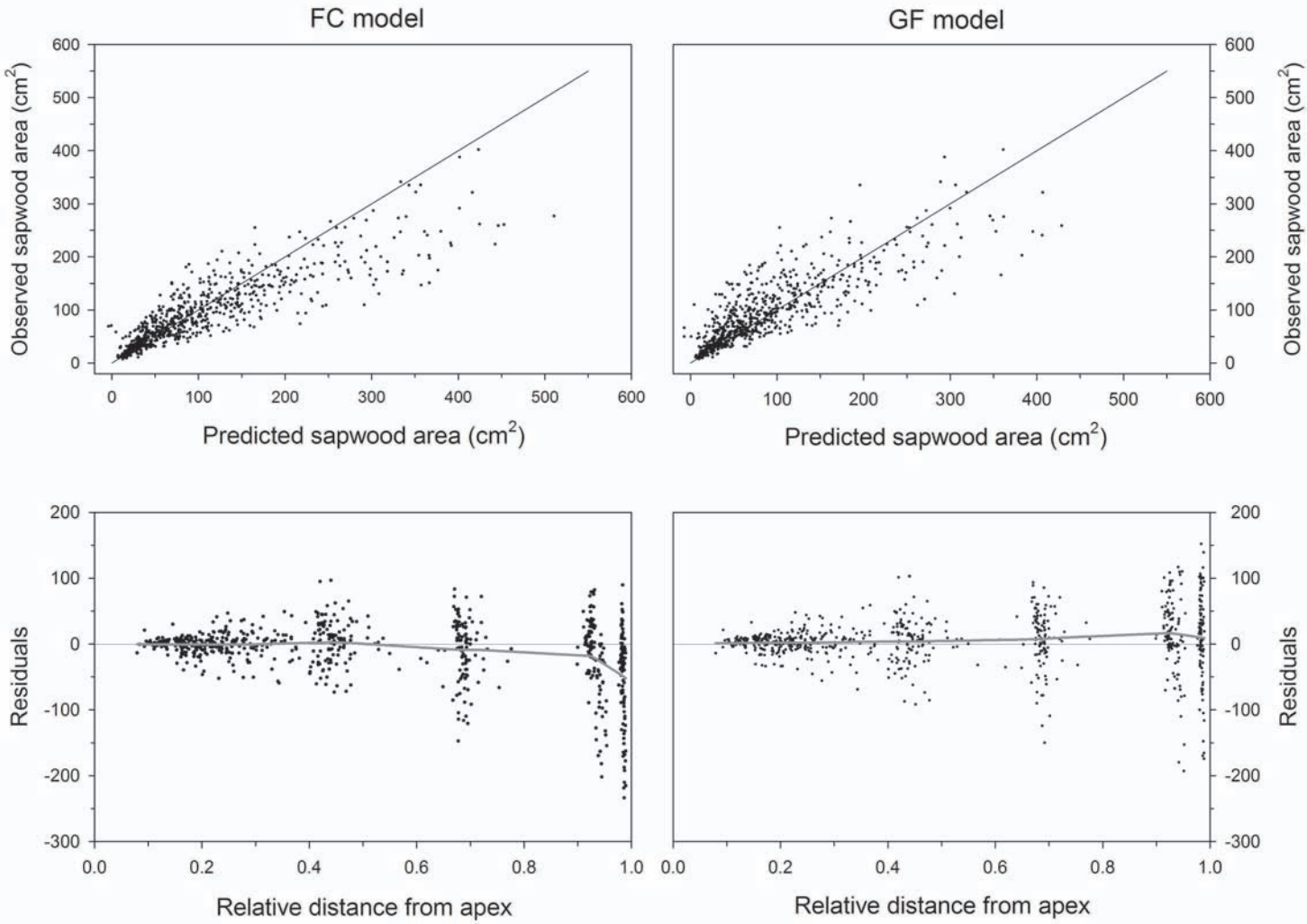
FC model
GF model
Observed sapwood area (cm^2)
Predicted sapwood area (cm^2)
Residuals
Relative distance from apex
0
100
200
300
400
500
600
-300
-200
-100
0.0
0.2
0.4
0.6
0.8
1.0